

# Role of Mitochondria in Cardiac Arrhythmias

by

Soroosh Solhjo

A dissertation submitted to Johns Hopkins University in conformity with the  
requirements for the degree of Doctor of Philosophy

Baltimore, Maryland

October, 2013

© 2013 Soroosh Solhjo

All Rights Reserved

# ABSTRACT

---

Mitochondria are the major organelles responsible for providing energy to the cardiac myocytes. In ischemic conditions, the supply of nutrients and oxygen to a region of the heart, or the whole organ, is interrupted. Reperfusion, while critically important for tissue survival, can cause more damage and can lead to arrhythmias and sudden cardiac death. Dysfunctional mitochondria are known to contribute to ischemia/reperfusion injury, but more specifically, spatiotemporal heterogeneity of recovery of mitochondrial energetics has been suggested to cause metabolic sinks of current, which act to either shorten the wavelength of, or block, the electrical excitation wave. In this thesis, I examine how the failure of mitochondrial energetics can lead to electrical irregularity and arrhythmias.

Monolayer cultures of neonatal rat ventricular myocytes were used for the experiments. Sarcolemmal voltage was recorded with optical mapping using the voltage-sensitive fluorescent dye, di-4-ANEPPS. Mitochondrial function was observed using the potentiometric fluorescent dye Tetramethyl Rhodamine Methyl Ester. Metabolic sinks were induced by chemically depolarizing mitochondria using a local perfusion system. Ischemia/reperfusion was modeled using a newly developed method of coverslip-induction of ischemia/reperfusion.

Regional depolarization of the mitochondrial network, either through the use of a chemical uncoupler or after ischemia/reperfusion of the monolayers, resulted in an increased propensity for arrhythmias. Reperfusion of the monolayer after one hour of ischemia initiated dynamic instability of the mitochondrial network consisting of

intracellular oscillations or global collapse of mitochondrial inner membrane potential ( $\Delta\Psi_m$ ) along with reentrant arrhythmias. Compounds which stabilized the mitochondria prevented reentry and electrical instability. Uncoupler-mediated regional depolarization of mitochondria to induce metabolic sinks also caused inexcitability and reentry, which were significantly prevented by pharmacological inhibition of ATP-sensitive  $K^+$  channels ( $K_{ATP}$ ).

Mitochondrial function is a major factor in determining the fate of an ischemic heart. In our *in vitro* model system, mitochondrial instability was demonstrated to be present during reperfusion and was highly correlated with electrical instability. Spatiotemporal heterogeneity in  $\Delta\Psi_m$  contributes to dispersion of repolarization and, in some cases, can also contribute to ectopic electrical activity. The results support the hypothesis that mitochondria are important targets for therapeutic intervention to prevent post-ischemic arrhythmias and sudden cardiac death.

Thesis readers:

Brian O'Rourke, PhD. Professor of Medicine. (Advisor)

Henry Reuben Halperin, MD. Professor of Medicine.

Thesis Committee Members:

Brian O'Rourke, PhD. Professor of Medicine. (Advisor)

Henry R. Halperin, MD. Professor of Medicine.

Joseph L. Greenstein, PhD. Assistant Research Professor of Biomedical Engineering.

Raimond L. Winslow, PhD. Professor of Biomedical Engineering.

*To my mother, Mehrangiz, for all the love, support, kindness, patience and advice.  
Counting the seconds to see her again.*

*To the memory of my beloved brother, Peyman, cherishing the best moments that we  
spent together.*

*And, to Salma, Mehran and Soheil, my sister and brothers.*

## Preface

Ischemic heart disease is the leading cause of death, responsible for the death of close to 375,000 out of 600,000 people who die of different types of heart disease each year, and more than 15.37% of total number of deaths annually in the United States alone<sup>1</sup>, costing the country \$108.9 billion a year<sup>2</sup>.

Ischemia, during occlusion of coronary arteries due to formation of a plaque, thrombosis or spontaneous spasm leads to a variety of changes in ion homeostasis, energetics and oxidative processes which contribute to mitochondrial and cellular injury. To decrease the ischemic damage and prevent cell death, reperfusion of the ischemic area is of key importance. However, reperfusion itself can lead to a more severe damage to this region, a phenomenon known as reperfusion injury<sup>3,4</sup>. In addition, there is a high chance of arrhythmias after reperfusion, which can be very dangerous and even cause sudden cardiac death<sup>5</sup>. A thorough understanding of the cellular and subcellular events implicated in ischemia and reperfusion is important to prevent their consequences.

A prominent feature of cardiac ischemia and reperfusion is the increase in the dispersion of refractoriness, one of the major mechanisms implicated in susceptibility to electrical instability and arrhythmias. The increase in dispersion of refractoriness is concurrent with depolarization of mitochondrial inner-membrane potential ( $\Delta\Psi_m$ ) and an increased spatiotemporal heterogeneity of energy metabolism<sup>6,7</sup>.

Mitochondria are the major consumers of oxygen and nutrients in cardiomyocytes, and the main producers of adenosine triphosphate (ATP) that is used by the energy-

consuming elements of the cell. Therefore, they are the first components of the cell that are affected by the lack of oxygen and nutrients of ischemic conditions. IR-induced metabolic stress on the mitochondrial network of the cardiomyocyte causes collapse or oscillation of the mitochondrial inner-membrane potential ( $\Delta\Psi_m$ )<sup>8</sup>. This leads to dissipation of energy, and increased accumulation of cellular reactive oxygen species (ROS).

Oxidative stress in a small number of mitochondria can spread to the whole mitochondrial network of a cardiomyocyte. Mitochondrial ROS-induced ROS release (RIRR) has emerged as a key event that underlies  $\Delta\Psi_m$  depolarization in cardiac cells<sup>9</sup>. RIRR refers to the autocatalytic production of a burst of ROS by the mitochondrial electron transport chain when mitochondria are subjected to exogenous sources of ROS, or when the antioxidant defenses of the mitochondrion or the cell are compromised<sup>10</sup>. This phenomenon can be synchronized across the entire mitochondrial network of the cardiomyocyte in a process that depends on local ROS diffusion and appears as a propagated  $\Delta\Psi_m$  depolarization wave<sup>11</sup>, or as sustained self-organized slow oscillations of  $\Delta\Psi_m$  (period  $\approx$  100 seconds)<sup>8,12</sup>. Further investigation on RIRR showed that ROS triggers the opening of an energy-dissipating ion channel<sup>8,10</sup>, known as the inner-membrane anion channel (IMAC)<sup>13,14</sup>. Opening of IMAC leads to uncoupling of mitochondria, resulting in rapid depolarization of  $\Delta\Psi_m$ , which transforms the mitochondria into consumers, rather than producers, of ATP through reverse activity of mitochondrial ATP synthase<sup>15</sup>, causing a drop in the cellular ATP/ADP ratio and loss of energy. The mechanisms linking mitochondrial dysfunction to electrical instability in the heart are incompletely understood.

The goal of the present study is to investigate the effects of IR on mitochondrial function, and the subsequent alterations of the dynamics of the electrophysiological substrate, which increase the vulnerability to arrhythmias resulting in the dysfunction of the whole heart. We use monolayer cultures of neonatal rat ventricular myocytes (NRVMs) as the experimental model. This provides a highly-controllable and easily-observable myocardial system to study mitochondrial function as well as electrical activity. The findings lend credence to the hypothesis that spatiotemporal mitochondrial instability underlies electrical instability during metabolic stress in the heart.



## **Acknowledgements**

I am most grateful to my dear advisor, Dr. Brian O'Rourke, for all the help, support, and friendship through these years. He spent a great amount of time and energy to train me and offered help and guidance whenever I faced an obstacle. It has been a great privilege to be a part of his lab, where I have also been fortunate with amazing labmates: Thomas Derungs, Roger Ortines, Robert Kazmierski, and Drs. Miguel Aon, Sonia Cortassa, Agnieszka Sidor, David Brown, Ting Liu, Lufang Zhou, Alice Ho, An-Chi Wei, Swati Dey, Roselle Abraham, Jackelyn Kembro, Tamara Zaobornyj, Rachael Carlisle, Celeste Villa-Abrille, and Niraj Bhatt.

I also like to thank my other friends and colleagues that helped me through this project; Mohammad Zauher and Dr. Rajish Sekar for teaching me primary cell isolation; Drs. Leslie Tung, Felipe Aguel, Debbie Castillo, and Miguel Valderrabano for technical advice and help. Thanks also to Dana Kemmer, Lisa Morales and Hong Lan for administrative assistance.

I also like to express my gratitude to my thesis committee members, Drs. Raimond Winslow, Joseph Greenstein, and Henry Halperin.

My deepest appreciations to all my family and friends for the love and support I have been receiving, without which I would not be able to achieve any of my goals.

## Table of Contents

Preface.....	vi
Table of Contents.....	x
List of Figures.....	xiv
1 Introduction.....	1
1.1 Mechanisms of Arrhythmias.....	1
1.2 Mitochondria in Ischemia/Reperfusion.....	3
1.3 Mitochondrial Criticality and RIRR.....	4
1.4 Dysfunction of mitochondria leads to shortened APs or inexcitability of the myocytes.....	7
1.5 Metabolic Sink Hypothesis.....	8
2 Metabolic Sinks Cause Reentry in NRVM Monolayers.....	11
2.1 Introduction.....	11
2.2 Methods.....	12
2.2.1 NRVM monolayers.....	12

2.2.2	Induction of Metabolic Sink .....	12
2.2.3	Optical Mapping of $V_m$ .....	14
2.2.4	Recording Mitochondrial Inner membrane Potential .....	14
2.3	Results .....	17
2.3.1	Effect of metabolic sink on action potential .....	17
2.3.2	Reentry due to metabolic sink.....	20
2.3.3	Size of Sink Area Affects the Outcome .....	21
2.3.4	$K_{ATP}$ Current: A Major Player in the Metabolic Sink Hypothesis .....	22
2.3.5	Antioxidant Depletion.....	23
2.4	Conclusion.....	26
3	Metabolic Sinks Form during Ischemia/Reperfusion .....	29
3.1	Introduction .....	29
3.2	Methods.....	31
3.2.1	NRVM Monolayers .....	31

3.2.2	Inducing Ischemia and Reperfusion.....	31
3.2.3	Recording $V_m$ .....	32
3.2.4	Measuring $\Delta\Psi_m$ .....	32
3.3	Results .....	33
3.3.1	Depolarization and Repolarization of Mitochondrial Inner-Membrane during IR .....	33
3.3.2	IR-Induced Arrhythmias .....	42
3.3.3	Effect of 4'-Cl-DZP on mitochondrial instability .....	45
3.3.4	Effect of 4'-Cl-DZP on reentry induced by reperfusion .....	49
3.3.5	Effect of Blocking $K_{ATP}$ channels during IR .....	49
3.4	Conclusion.....	52
4	Discussion and Conclusions.....	55
4.1	Considerations.....	58
4.2	Future Direction: Effect of Inhibition of Mitochondrial $Na^+/Ca^{2+}$ Exchanger on IR-Induced Reentry .....	60

4.2.1	Objective and Methods .....	60
4.2.2	Results and Conclusion.....	61
4.3	Future Direction: Monolayers of Adult Cardiomyocytes .....	65
4.4	Future Direction: Genetic Manipulation of Sarc-/Mito-K <sub>ATP</sub> Channels .....	66
	Bibliography .....	67
	Curriculum Vitae .....	76

## List of Figures

Figure 1 Scaling from a mitochondrion to the whole heart. ....	4
Figure 2 $K_{ATP}$ is sensitive to ATP/ADP.....	8
Figure 3 Metabolic sinks and arrhythmia. ....	9
Figure 4 Local perfusion lid.....	13
Figure 5 The user interface of the optical mapping software for acquiring data. ....	15
Figure 6 The user interface of the optical mapping software for producing the movie....	16
Figure 7 FCCP depolarizes the mitochondria. ....	17
Figure 8 Mitochondrial depolarization and propagation of excitation wave. ....	18
Figure 9 Action potential during FCCP perfusion and washout. ....	18
Figure 10 Effect of FCCP on action potential amplitude and duration at 37°C. ....	19
Figure 11 Effect of FCCP on Action Potential at room temperature.....	19
Figure 12 Sustained reentry during perfusion with FCCP.....	20
Figure 13 Transient reentry during washout of FCCP.....	21

Figure 14 Glibenclamide modifies the effects of FCCP.....	22
Figure 15 Effect of glibenclamide on FCCP-induced inexcitability (room temperature). 23	
Figure 16 Effect of diamide on $\Delta\Psi_m$ .....	24
Figure 17 Effect of diamide on APA.....	25
Figure 18 Reentry, 6 minutes after washout of diamide.....	26
Figure 19 $\Delta\Psi_m$ at 5 minutes and 1 hour of ischemia.....	34
Figure 20 Effect of 1 hour ischemia on the $\Delta\Psi_m$ .....	34
Figure 21 First phase of mitochondrial depolarization due to ischemia.....	35
Figure 22 Effect of long-term ischemia on $\Delta\Psi_m$ .....	37
Figure 23 Wave of depolarization of $\Delta\Psi_m$ during ischemia.....	38
Figure 24 Change of $\Delta\Psi_m$ during ischemia and reperfusion.....	39
Figure 25 Oscillation of $\Delta\Psi_m$ upon reperfusion.....	40
Figure 26 Oscillations of adjacent clusters are synchronized during early reperfusion. ....	41
Figure 27 Coverslip-induced ischemia affects the propagation of the excitation wave. ...	43

Figure 28 Electrical propagation during reperfusion.....	44
Figure 29 Effect of different chemicals on ischemia-induced mitochondrial depolarization.....	46
Figure 30 4'-Cl-DZP stabilizes the mitochondria.....	47
Figure 31 PTP involvement in large-scale reperfusion-induced mitochondrial $\Delta\Psi_m$ loss. .....	48
Figure 32 4'-Cl-DZP stabilizes electrical activity.....	51
Figure 33 Effect of $K_{ATP}$ inhibition on mitochondrial instability.....	52
Figure 34 $[Ca^{2+}]_m$ during IR in control and NCLX-overexpressed monolayers.....	62
Figure 35 $[Ca^{2+}]_c$ during coverslip-induced IR.....	63
Figure 36 Changes in the pH of the cardiac cells during IR.....	64
Figure 37 Electrical activity of the monolayer in presence of CGP.....	65



# 1 Introduction

Here, we review the alterations in mitochondrial function and subsequent changes in cellular and organ level activity of the heart muscle during IR. We will introduce the hypothesis of metabolic sinks of current as a mechanism promoting IR-induced arrhythmias.

## 1.1 Mechanisms of Arrhythmias

Several arrhythmogenic mechanisms have been proposed to be involved in ischemia/reperfusion (IR)-induced arrhythmias (see ref.<sup>16</sup>). Under normal conditions, the heart beat is controlled by the fastest pacemaker in the heart, i.e., the sinoatrial (SA) node. However, in pathological situations, such as IR, the firing rate of other pacemakers might increase due to high sympathetic stimulation<sup>17</sup>; or ectopic pacemakers, e.g. on the border zone of the ischemic area, might disturb the normal rhythm of the heart<sup>18</sup> and arrhythmias happen due to abnormal automaticity. Mechanisms for triggered activity in non-pacemaker cells include early- and delayed- afterdepolarizations (EAD and DAD, respectively). If the action potential (AP) plateau becomes long enough, the L-type  $\text{Ca}^{2+}$  channels may recover from inactivation, allowing these channels to open again and trigger an EAD<sup>19</sup>. Under certain conditions, such as  $\text{Na}^+$  overload<sup>20</sup>, spontaneous  $\text{Ca}^{2+}$  release from the SR during diastole can cause activation of transient inward currents (through the  $\text{Na}^+$ - $\text{Ca}^{2+}$  exchanger or nonspecific  $\text{Ca}^{2+}$ -activated channels) in the sarcolemma, resulting in depolarization of the resting membrane potential, i.e., a DAD. If

the DAD is large enough, the membrane potential may exceed the threshold for triggering a spontaneous AP. EADs and DADs can thus be important arrhythmogenic mechanisms during IR. Other arrhythmogenic mechanisms can also be involved in IR-related arrhythmias, including dispersion of refractoriness, slowed conduction velocity (CV), or regional excitation block. These latter alterations can favor reentry.

Reentrant arrhythmias are a common type of cardiac arrhythmia<sup>21</sup>. Reentry is the recurrent excitation of a part of the muscle tissue with the same excitation wave. In the normal situation, each excitation wave is elicited from SA node in the right atrium, and after a short delay at the atrioventricular (AV) node, propagates through the cardiac His-purkinje conduction system to activate the ventricles in a coordinated manner. This normal propagation is needed for effective excitation and contraction of heart. In reentry, an excitation wave, arising either from the conduction system or from a site of ectopic activity, does not terminate and returns to previously excited areas. If these regions have recovered from the refractory state, reentry can be initiated, usually at a frequency much higher than the normal heart beat, resulting in tachycardia or fibrillation. The resulting uncoordinated contraction of the myocardium does not support effective ejection of the blood and cardiac output decreases below that required to sustain circulation to the rest of the body.

In reentry, the excitation wave propagates through a circuitous pathway which is formed around an anatomical or functional obstacle. Anatomical obstacles are parts of the heart tissue that are not excitable, e.g. scar tissue. Functional obstacles, however, are formed due to heterogeneity of the electrophysiological properties of the tissue. Usually, a

transient unidirectional block, e.g., due to refractoriness, causes the excitation wave to turn around the obstacle and form a reentrant wave. For reentry to happen, the length of the pathway should be long enough so that the second time the excitation wavefront reaches a point, that point is excitable and not refractory. Therefore, slow conduction velocity and dispersion of the refractory period promote reentry. Changes in resting membrane potential during IR can contribute to both abnormal conduction velocity and dispersion of refractoriness. Many other factors, such as gap junctional uncoupling or changes in ionic concentrations can also be involved in mechanisms leading to formation of reentrant waves. For more information on reentry and subsequent cardiac fibrillation please refer to ref<sup>22</sup>.

## **1.2 Mitochondria in Ischemia/Reperfusion**

IR-induced changes in ion gradients and their effects on resting membrane potential and the action potential of the cell can occur through direct and indirect mechanisms involving ion channels and transporters on both the sarcolemmal and mitochondrial membranes. The interaction between the altered ion fluxes across these two compartments could be a main factor that drives arrhythmias, especially when these changes occur in a heterogeneous manner. Failure of the mitochondrial network of cardiac myocytes to produce energy, to control the amount of reactive oxygen species (ROS), to prevent proton accumulation, and to regulate ion concentrations ( $\text{Na}^+$  and  $\text{Ca}^{2+}$ )

are key factors in the vast number of changes at the cellular and subcellular level that can scale to organ level electrical and contractile dysfunction (Figure 1).

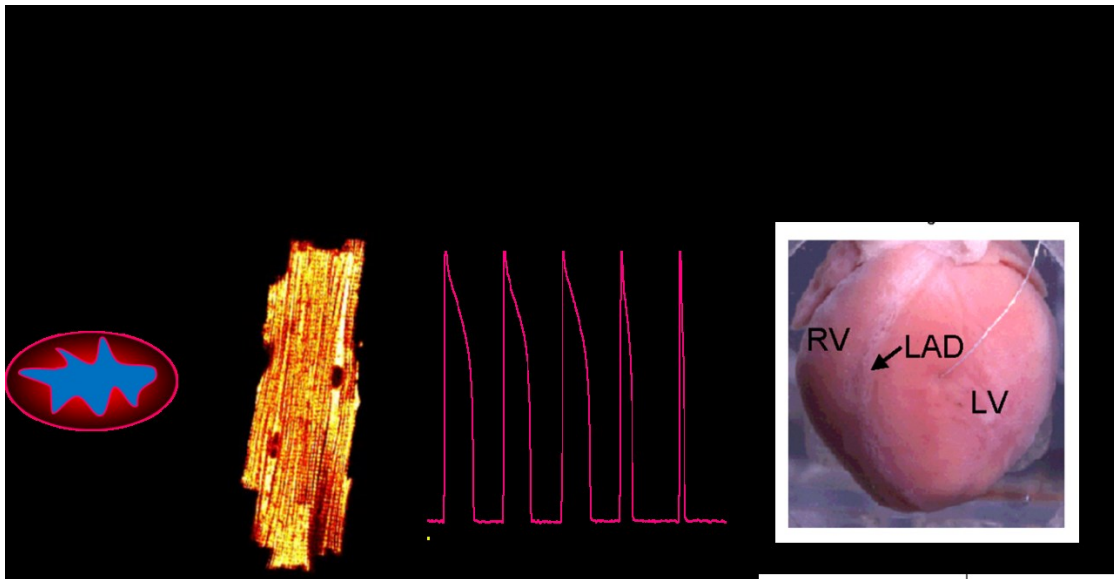


**Figure 1 Scaling from a mitochondrion to the whole heart.**

**Changes in function of an individual mitochondrion scales to changes in the mitochondrial network of the cardiomyocyte, to cellular activity, and to the contractile and electrical function of the whole heart.**

### **1.3 Mitochondrial Criticality and RIRR**

If oxidative stress exceeds a threshold in the majority of mitochondria in an isolated cardiomyocyte, a state called mitochondrial criticality may be reached<sup>12,23</sup>. A

mitochondrial network in the critical state becomes hypersensitive to small perturbations, and depolarization of a few mitochondria, or even one, can lead to propagation of a wave of  $\Delta\Psi_m$  depolarization and collapse, or oscillation, of the whole network<sup>11,12,24</sup>.

Spread of the mitochondrial instability or depolarization wave through the whole mitochondrial network is through an autocatalytic mechanism called ROS-induced ROS-release (RIRR)<sup>9,25,26</sup>. RIRR was originally demonstrated by increased ROS generation via photodynamically-induced mitochondrial depolarization<sup>9</sup>. However, an increase in mitochondrial ROS generation due to inhibition of scavenging systems can cause a similar effect<sup>10</sup>. When ROS in a mitochondrion increases by a certain amount, the mitochondrion loses its inner membrane potential, due to opening of energy-dissipating channels, and becomes depolarized. The resulting depolarization itself causes a burst of mitochondrial ROS generation by the electron transport chain. Release of ROS would affect the neighboring mitochondria and will enhance their ROS generation, essentially propagating mitochondrion-to-mitochondrion RIRR. This will cause their depolarization and further ROS release. This process continues to spread until the whole mitochondrial network is depolarized or oscillates synchronously. RIRR might also spread to the mitochondria of neighboring cells and ultimately affect the whole tissue. In its initial description, activation of the permeability transition pore (PTP) was suggested as the main mechanism of RIRR<sup>9</sup>. RIRR was shown to be inhibited by bongkreikic acid, an inhibitor of the adenine nucleotide translocase, thought to be a regulator of PTP, and evidence for calcein permeability of the inner membrane was reported. However, Cyclosporine A (CsA), a PTP inhibitor, could not prevent RIRR induced by laser excitation<sup>9</sup>. Work from the O'Rourke group revealed that RIRR also underlies self-

sustained cell-wide mitochondrial oscillations in adult cardiomyocytes<sup>8</sup> triggered either by energy substrate depletion, highly localized laser excitation, or glutathione depletion. These oscillations were insensitive to CsA, independent of cell  $\text{Ca}^{2+}$ , and did not involve large scale permeability changes in the inner membrane. Furthermore, they were effectively blocked by ligands of peripheral benzodiazepine receptors, leading to an alternative mechanistic explanation for RIRR involving ROS-sensitive inner membrane anion channels (IMAC). Therefore, IMAC was introduced as a major player in mitochondrial instability resulting from oxidative stress<sup>8</sup>.

A mitochondrial benzodiazepine receptor with nanomolar affinity is known to exist on the mitochondrial outer membrane, but IMAC was originally proposed to be present on the inner membrane of mitochondria<sup>14</sup>, with micromolar sensitivity towards ligands of the mitochondrial benzodiazepine receptor (mBZR). Intriguingly, a benzodiazepine modulated ion channel on the inner membrane has also been described by several groups<sup>27</sup>, but its molecular structure has yet to be deduced. For the purposes of this thesis, we will use IMAC to refer to the energy-dissipating inner membrane channel activated by ROS and blocked by 4'-Cl-Diazepam (4'-Cl-DZP), but not CsA, that underlies  $\Delta\Psi_m$  loss under oxidative stress. 4'-Cl-DZP was shown to stabilize stressed mitochondria and prevent depolarization and oscillation of  $\Delta\Psi_m$ <sup>8,28</sup>. Moreover, 4'-Cl-DZP also inhibited AP oscillations linked to  $\Delta\Psi_m$  oscillation, as well as reperfusion arrhythmias<sup>28</sup>.

## **1.4 Dysfunction of mitochondria leads to shortened APs or inexcitability of the myocytes**

$\Delta\Psi_m$  is established by proton pumping action of the mitochondrial electron transport chain. The electrochemical gradient for protons (the protonmotive force) then drives the mitochondrial ATP synthase to produce ATP from ADP<sup>29</sup>. Mitochondrial depolarization leads to loss of ATP production and also induces fast ATP consumption through reverse activity of the ATP synthase<sup>15</sup>, thereby dramatically decreasing the ATP/ADP ratio. One of the major sensors of ATP in the cell is the ATP-sensitive K<sup>+</sup> channel (K<sub>ATP</sub>) (Figure 2). A decrease in ATP/ADP will activate sarcolemmal K<sub>ATP</sub> channels and induce a large background potassium current<sup>30,31</sup> that decreases excitability. Opening of sarcolemmal K<sub>ATP</sub> channels mediates a steady outward current of K<sup>+</sup> during the AP plateau, accelerating repolarization to shorten the action potential duration (APD). A large K<sub>ATP</sub> current can also render the cell inexcitable<sup>28</sup>. Inward excitation current through fast Na<sup>+</sup> channels will be opposed by outward K<sub>ATP</sub> current, effectively increasing the threshold for AP firing. This “current sink” effect is the basis of the metabolic sink hypothesis of arrhythmias<sup>28</sup>.

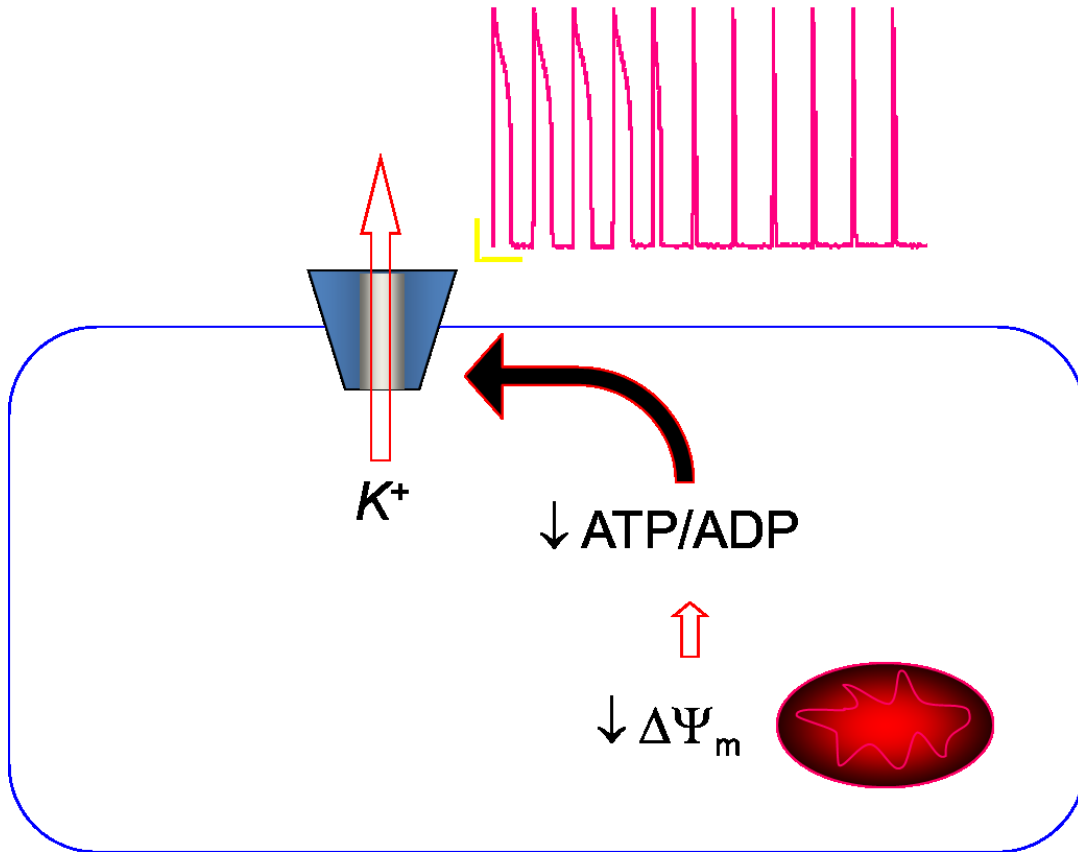


**Figure 2**  $K_{ATP}$  is sensitive to ATP/ADP.

**When ATP/ADP reaches a threshold low value,  $K_{ATP}$  channels open and establish a large  $K^+$  current across the sarcolemmal membrane which shortens the APD and lowers excitability of the myocyte.**

### **1.5 Metabolic Sink Hypothesis**

Metabolic stress during ischemia and upon reperfusion is a major effect of IR on cardiomyocytes, rendering their mitochondrial network unstable. Mitochondrial dysfunction shortens the AP and lowers the excitability of the cardiac myocytes, and if



this occurs heterogeneously in the myocardium, the conduction pathway and wavelength of electrical excitation can be strongly impacted. Metabolic sinks of the excitation current and could act as functional blocks in front of the propagating excitation wave, or else act to markedly shorten the waves, resulting in regions of tissue with very short refractory periods next regions with longer refractory periods. Changes in the pathlength, together with the large increase in dispersion of repolarization then could promote reentry and cause whole heart arrhythmias<sup>28</sup> (Figure 3).

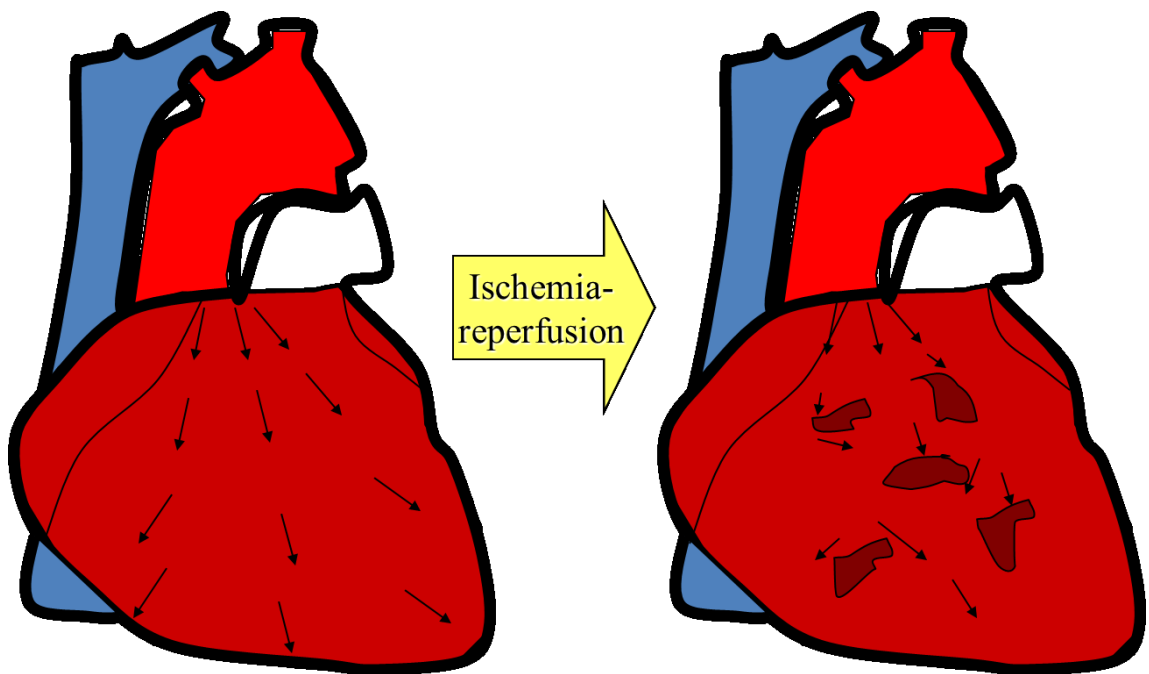


**Figure 3 Metabolic sinks and arrhythmia.**

**Formation of metabolic sinks due to IR can provide reentrant circuits and lead to arrhythmia.**

The goal of this project is to test the metabolic sink hypothesis in monolayers of neonatal rat ventricular myocytes (NRVM), a 2D experimental model of heart tissue. Advantages of using a monolayer include the possibility of highly precise observation of mitochondrial and electrical function and the fact that the preparation is more homogeneous than the whole heart, allowing for the selective induction of a defined metabolic sink in a controlled region of the monolayer.

## 2 Metabolic Sinks Cause Reentry in NRVM Monolayers

### 2.1 Introduction

Based on experiments with ischemic whole hearts, Akar *et al.* hypothesized that metabolic stress due to IR would cause  $\Delta\Psi_m$  instability and the formation of metabolic sinks<sup>28</sup>. Spatiotemporal heterogeneity of the electrical substrate would then provide the conditions that promote reentrant arrhythmias.

To test this hypothesis, we first study the effects of induction of a metabolic sink on propagation of an excitation wave. We examine whether the presence of metabolic sinks can lead to occurrence of reentry in monolayer cultures of neonatal rat ventricular myocytes (NRVM). We induce a metabolic sink in NRVM monolayers by uncoupling the mitochondrial electron transport chain using a chemical protonophore, which dissipates  $\Delta\Psi_m$  and results in ATP consumption. Local mitochondrial uncoupling in only one part of the monolayer was accomplished by perfusing the center part of the monolayer with the chemical uncoupler, while the cells outside of this zone were perfused with normal physiological solution. By means of optical mapping, we observed how mitochondrial depolarization affects the electrical activity and propagation of excitation waves through the monolayers.

## **2.2 Methods**

### **2.2.1 NRVM monolayers**

Dissection was performed on 2-day old newborn Sprague-Dawley rats (Harlan Laboratories); their ventricles were excised, chopped into small pieces, washed with HBSS and then put overnight in a solution of trypsin in HBSS in the cold room at 4 °C. The procedure conformed to the protocols of the National Institutes of Health<sup>32</sup>.

The next day, the cardiomyocytes were isolated using collagenase. Two preplating procedures were done to reduce the fibroblast concentration and then cells were suspended in Medium 199 (Invitrogen), supplemented with 10% heat-inactivated fetal bovine serum (Invitrogen). 850,000 cells were plated on each plastic coverslip (D = 2.1 cm), coated with fibronectin (25 µg/mL). After one day, serum was reduced to 2%. After 5-7 days in culture, beating and confluent monolayers were used for experiments.

### **2.2.2 Induction of Metabolic Sink**

To create a metabolic sink, the center part of the monolayer was perfused, using a custom-made local perfusion device<sup>33</sup> (Figure 4), with Tyrode's solution (see below) containing the mitochondrial oxidative phosphorylation uncoupler, carbonyl cyanide-p-trifluoromethoxyphenylhydrazone (FCCP, 1 µM; Sigma-Aldrich). The rest of the monolayer received only normal Tyrode's solution. FCCP was used to depolarize the

mitochondria and generate a metabolic sink without inducing extensive oxidative modifications of ion channels and transporters.

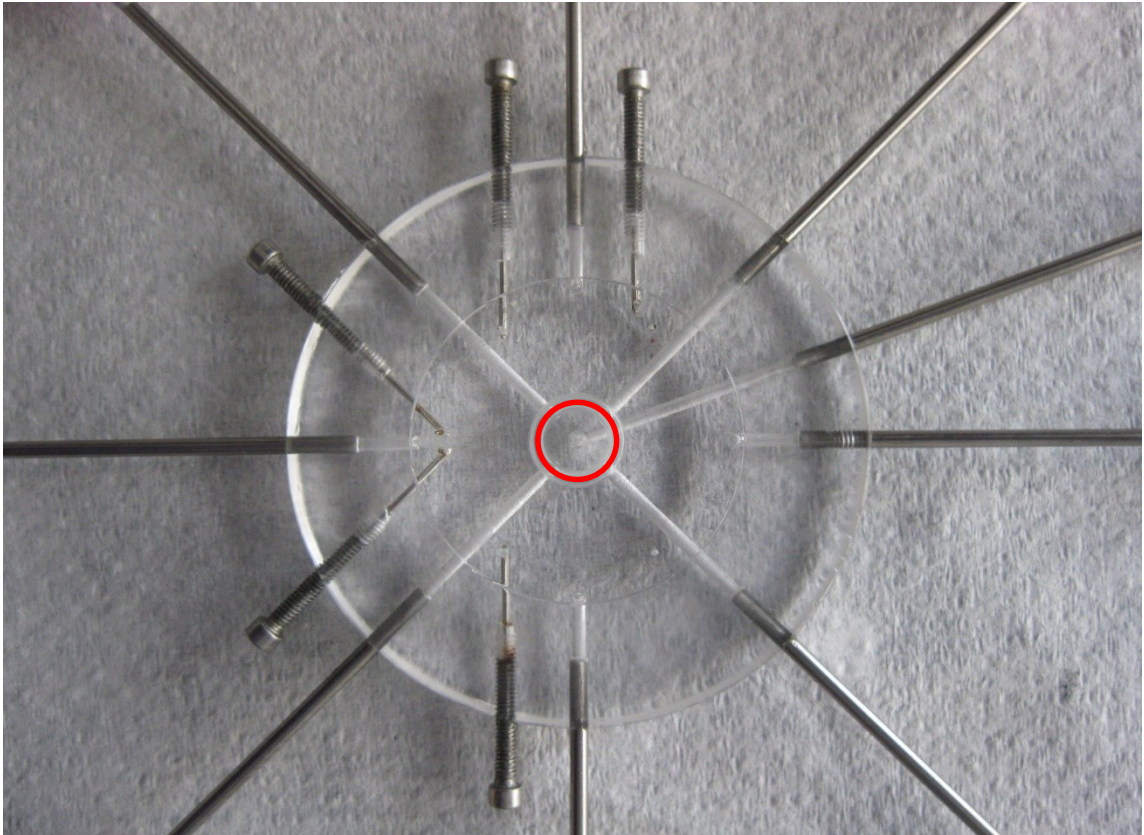


**Figure 4 Local perfusion lid.**

**The center part (shown with a red circle) receives FCCP-containing solution while the outer part receives only normal physiological solution.**

### **2.2.3 Optical Mapping of $V_m$**

To observe the changes in sarcolemmal membrane potential, the monolayers were stained with 5  $\mu\text{mol/l}$  di-4-ANEPPS (Invitrogen) for 15-30 minutes in the 37 °C incubator, then they were washed and put in the custom-built chamber of the optical mapping setup and continuously superfused with Tyrode's solution consisting of (in mM) 135 NaCl, 5.4 KCl, 1.8 CaCl<sub>2</sub>, 1 MgCl<sub>2</sub>, 0.33 NaH<sub>2</sub>PO<sub>4</sub>, 5 HEPES, and 5 glucose, unless noted otherwise. The chamber was maintained at 37 °C. Excitation light of  $480 \pm 15$  nm was used and emitted fluorescence was recorded at 500 Hz, with a 464-element photodiode array (WuTech), after passing through a red dye-coated glass filter (605nm; long-pass). After filtering and digitization, data was analyzed with software developed using LabVIEW (Texas Instruments) and MATLAB (MathWorks). Basic processing included zero-phase application of low-pass and high-pass butterworth filters, median filtering, detrending, normalization and application of a spatial filter. Filter order, cutoff frequencies, order of median filter and spatial filter were all adjustable by the user through the graphical user interface; the default values are 1, 0.1 Hz – 25 Hz, 7 and 1 respectively. The graphical user interface can be seen in Figure 5 and Figure 6.

### **2.2.4 Recording Mitochondrial Inner membrane Potential**

Regional  $\Delta\Psi_m$  depolarization by local FCCP perfusion was recorded using the potentiometric fluorescent indicator tetramethylrhodamine methyl ester (TMRM, 2  $\mu\text{M}$ ) in the dequench mode<sup>34</sup>. In this mode, the TMRM concentration in the mitochondrial

matrix exceeds a critical level above which its fluorescence self-quenches. Consequent depolarization of  $\Delta\Psi_m$  is then indicated by an increase in fluorescence due to dequenching. After TMRM was loaded for 1 hour, the monolayer was imaged from above by means of a cooled CCD camera (MicroMax 1300Y; Princeton Instruments).

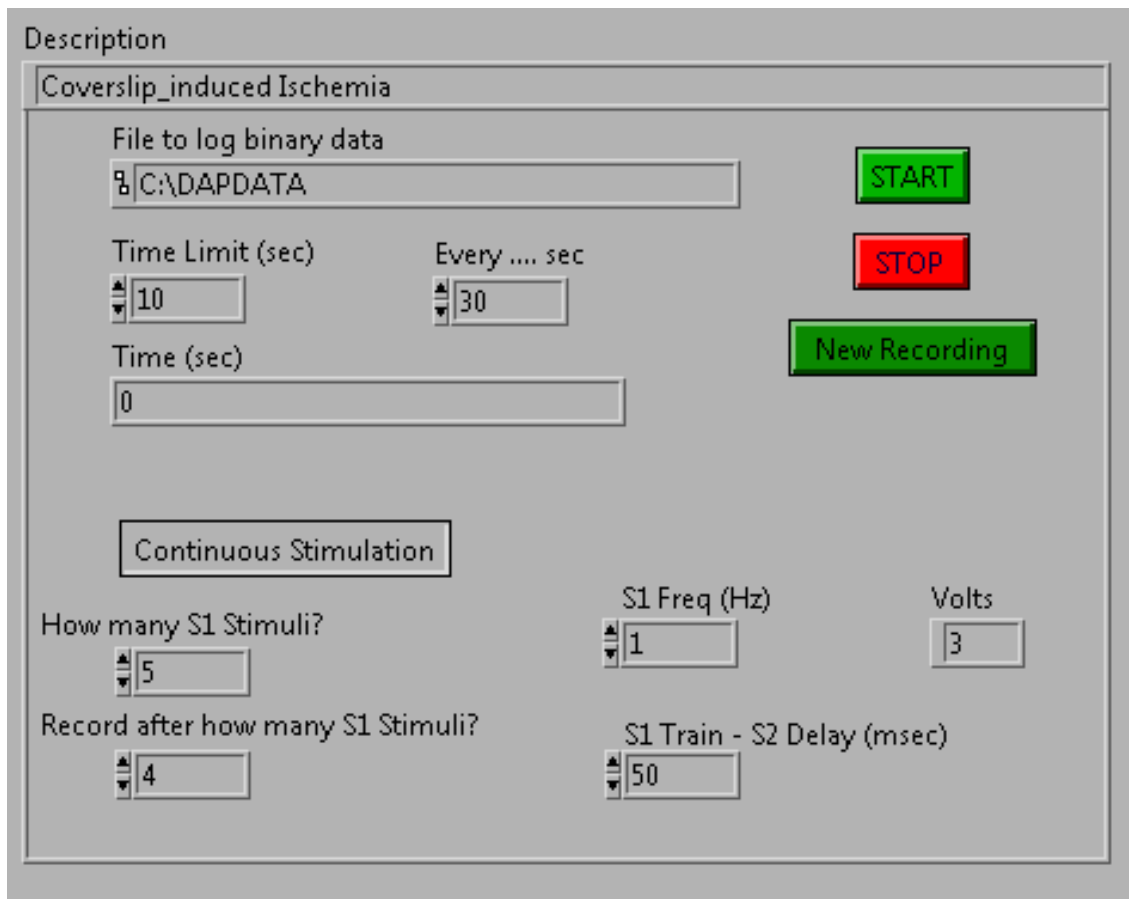


Figure 5 The user interface of the optical mapping software for acquiring data.

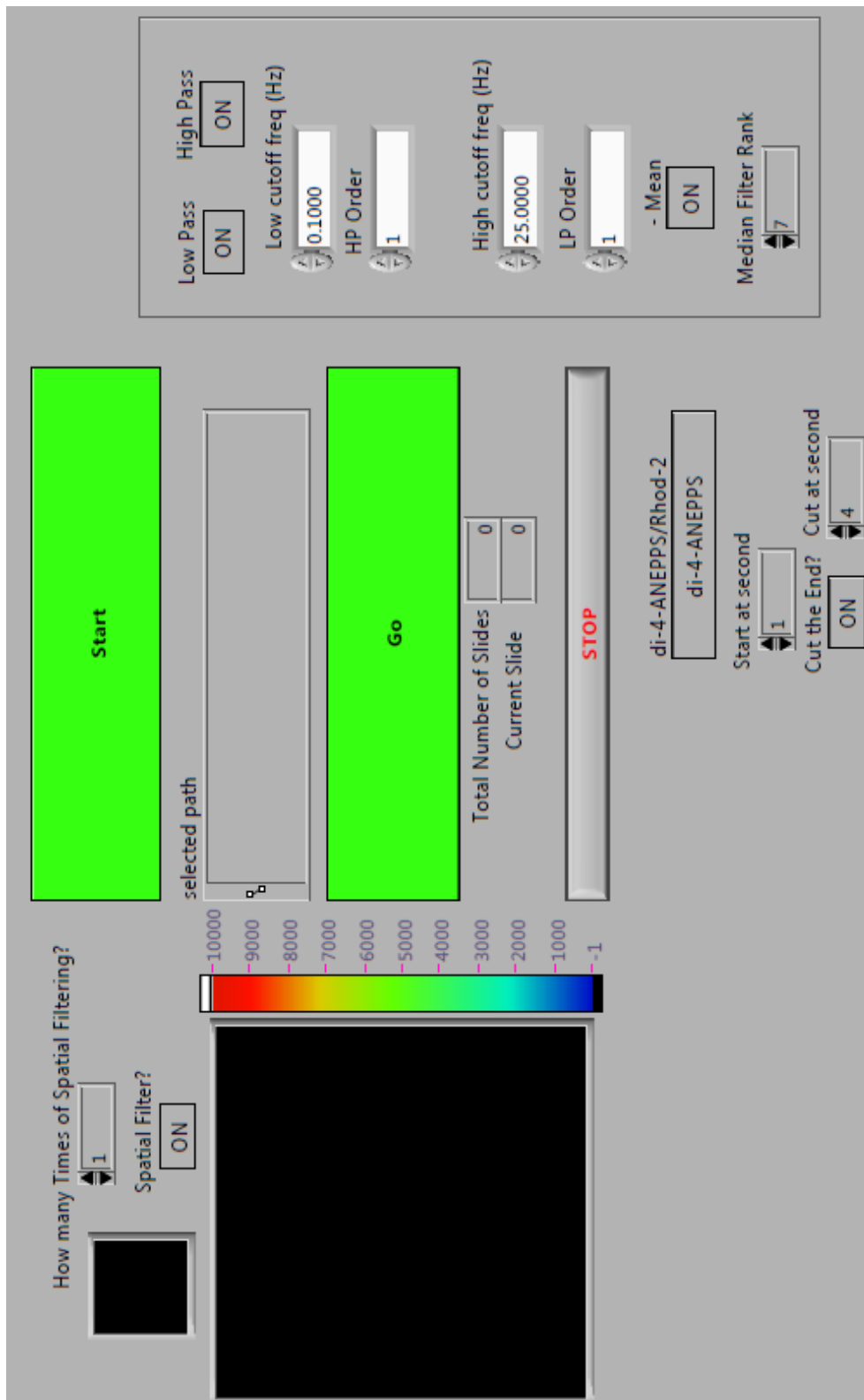
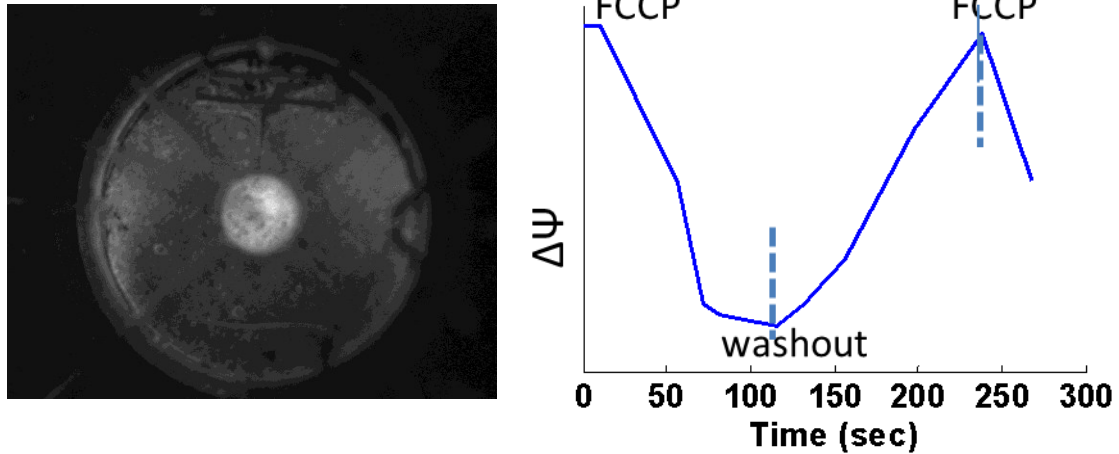


Figure 6 The user interface of the optical mapping software for producing the movie.



## 2.3 Results

Local perfusion of the center part ( $D = 0.5$  cm) of the monolayer with FCCP-containing solution induced regional  $\Delta\Psi_m$  depolarization (Figure 7).



**Figure 7 FCCP depolarizes the mitochondria.**

Local perfusion with FCCP depolarizes the mitochondria of the cells in the center zone of the monolayer. Upper: TMRM in dequench mode. Lower: Changes in  $\Delta\Psi_m$  in the center zone in response to FCCP perfusion or washout.

### 2.3.1 Effect of metabolic sink on action potential

As a consequence of  $\Delta\Psi_m$  depolarization, wavelength shortened and wave slowing was observed (Figure 8). Mitochondrial depolarization also resulted in a fast decrease in both

APA and APD<sub>50</sub> (Figure 9, Figure 10). Effect of FCCP on the action potential was observed to be much slower at room temperature (Figure 11).

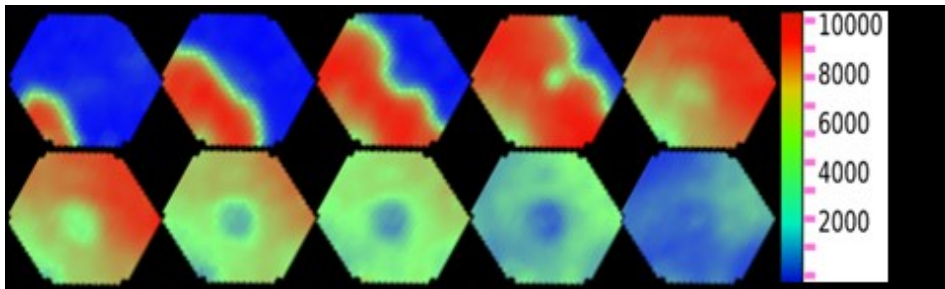


**Figure 8 Mitochondrial depolarization and propagation of excitation wave.**

Loss of  $\Delta\Psi_m$  decreased APA and APD, resulting in wavefront slowing and a shorter refractory period within the metabolic sink. Bipolar point stimulation at 1 Hz; frame rate: 50 Hz.

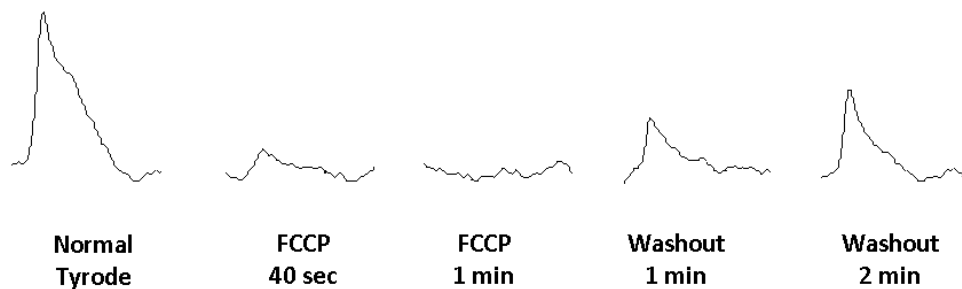


**Figure 9 Action potential during FCCP perfusion and washout.**

Mitochondrial uncoupling and subsequent depolarization causes inexcitability. Cardiomyocytes recover upon reperfusion.

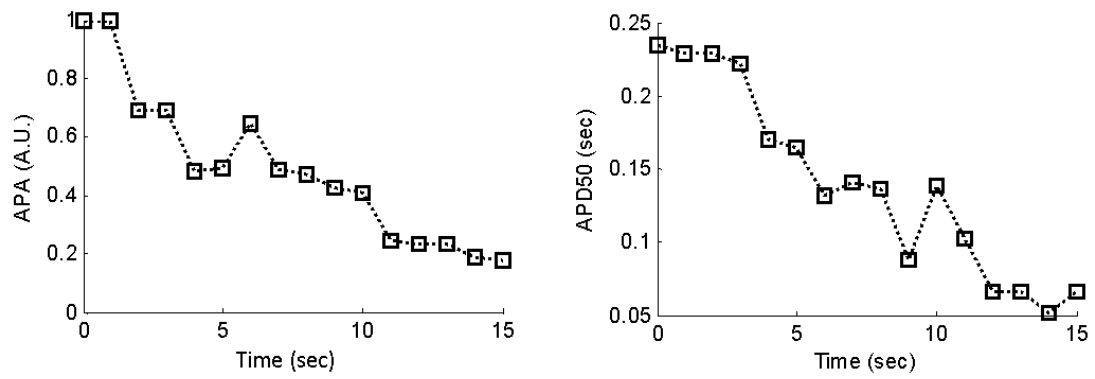


Figure 10 Effect of FCCP on action potential amplitude and duration at 37°C.

The sink area becomes inexcitable in less than a minute.

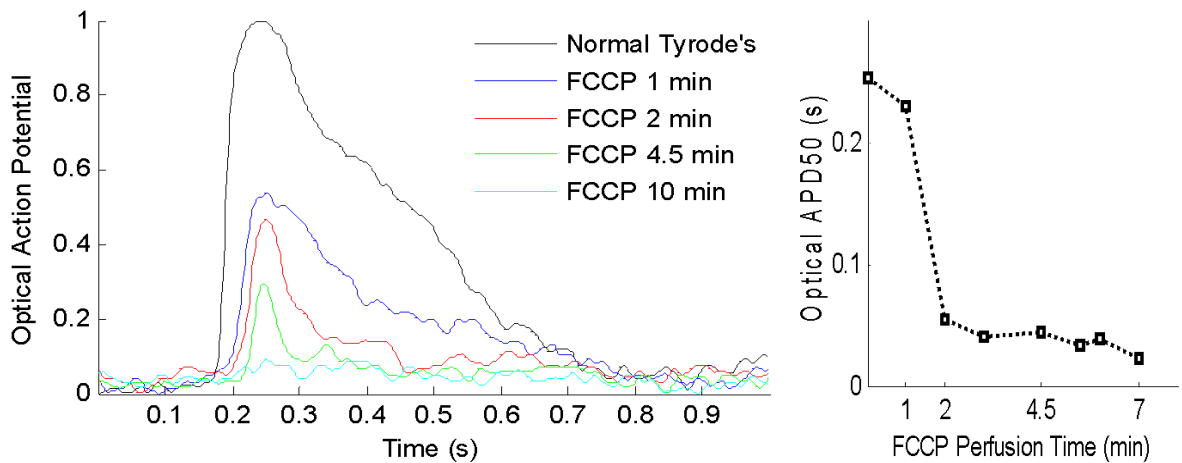


Figure 11 Effect of FCCP on Action Potential at room temperature.

At room temperature, it takes ~10 minutes for FCCP to render the sink area inexcitable.

### 2.3.2 Reentry due to metabolic sink

Induction of a metabolic sink elicited wavebreaks and occasionally led to formation of reentry. Figure 12 shows such an event in a monolayer paced at 4 Hz. Spiral waves formed and continued for several minutes after pacing was turned off. Also, heterogeneity in refractoriness and conduction, due to reperfusion of the metabolic sink with normal physiological solution to restore  $\Delta\Psi_m$ , caused transient or sustained reentry. Figure 13 shows formation of a transient reentrant wave in a monolayer, as the sink started to regain excitability upon FCCP washout.

Overall, reentry occurred in 6 out of 10 monolayers paced at 1-4 Hz (4 monolayers during FCCP perfusion and 4 during washout).

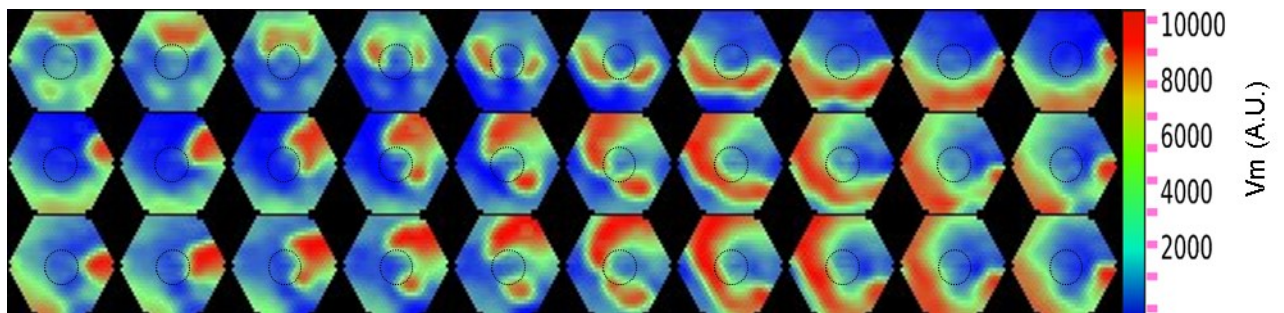
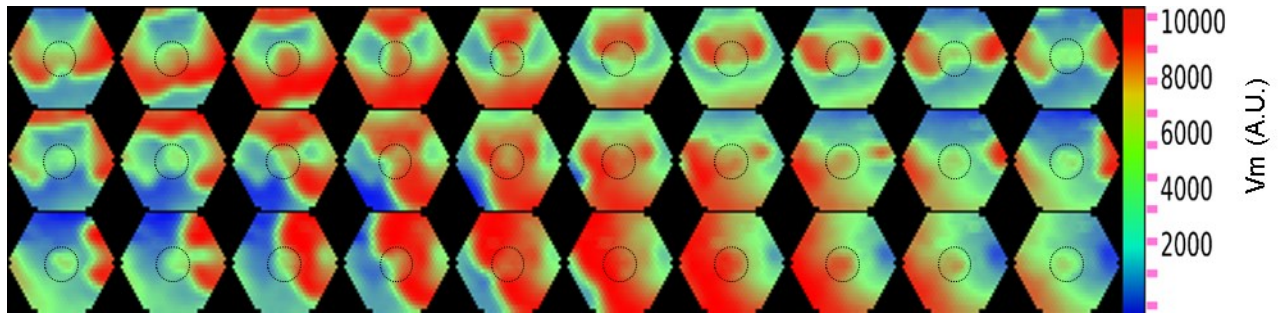


Figure 12 Sustained reentry during perfusion with FCCP.

Dotted circles show the approximate border of the metabolic sink. Bipolar point stimulation at 4 Hz; frame rate: 33 Hz.



**Figure 13** Transient reentry during washout of FCCP.

Dotted circles show the approximate border of the metabolic sink. Bipolar point stimulation at 4 Hz; frame rate: 25 Hz.

### 2.3.3 Size of Sink Area Affects the Outcome

To study the effect of sink size on the occurrence of reentry, in another set of experiments (21 monolayers), a larger area ( $D = 1.2$  cm) of the monolayer was perfused with FCCP and thus a larger metabolic sink was induced. Reentry occurred during FCCP perfusion in response to an S2 stimulus ( $S1-S2 = 200$  ms), applied on the border of the sink, in monolayers with the large sink size (3 out of 3 monolayers). An extrastimulus at the border of the sink area did not cause reentry in any monolayer with the small sink. In the absence of S2 stimulus, spontaneous activity occasionally initiated close to the edge of the sink and led to reentry when the monolayer was paced at 1 Hz (2 out of 18 monolayers).

### 2.3.4 $K_{ATP}$ Current: A Major Player in the Metabolic Sink Hypothesis

In the presence of glibenclamide, a blocker of  $K_{ATP}$  channels, the APA decrease was blunted and APD shortening was mostly prevented (Figure 14). Consequently, in contrast to FCCP perfusion alone, glibenclamide prevented complete inexcitability of the sink area. Transient reentry occurred for 1-2 minutes only in 2 out of 6 monolayers (1 monolayer during FCCP perfusion and 1 during washout). Glibenclamide also increased APD during washout of FCCP. The effect of glibenclamide was even more evident at room temperature, where it almost completely eliminated APD shortening (Figure 15).

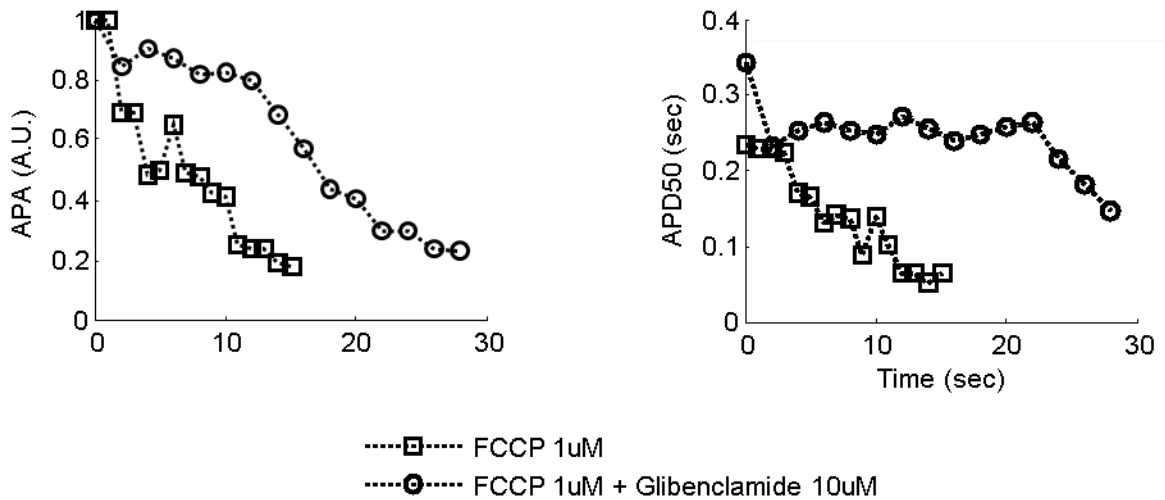


Figure 14 Glibenclamide modifies the effects of FCCP.

Glibenclamide (10  $\mu$ M) prevented rapid APD shortening and blunted APA decrease. Perfusion with FCCP starts at time 0. Bipolar point stimulation was applied at 1 Hz.

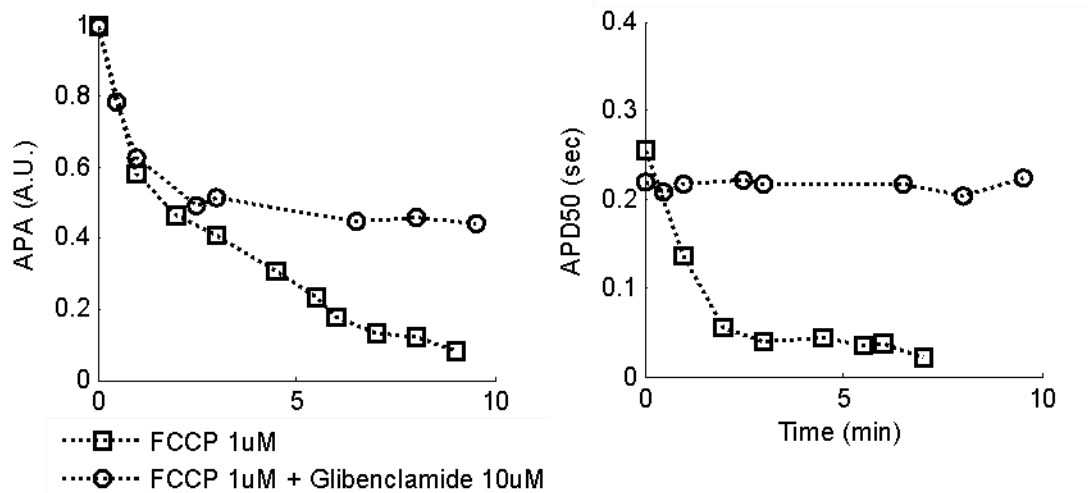


Figure 15 Effect of glibenclamide on FCCP-induced inexcitability (room temperature).

Effect of local perfusion with FCCP (1  $\mu$ M) on optically measured APA and APD<sub>50</sub> in the sink area with/without glibenclamide (10  $\mu$ M) at room temperature are much more discernible.

### 2.3.5 Antioxidant Depletion

In another set of experiments, we locally perfused the center part of the monolayer with diamide to deplete the GSH pool and induce oxidative stress<sup>10</sup>, which, in turn, led to mitochondrial depolarization (Figure 16). As a result of perfusion with diamide at 1mM, APA decreased (Figure 17). Reentry occurred in 2 out of 3 monolayers upon washout of diamide; however, unlike FCCP, the inexcitable area did not recover (even when washout with normal Tyrode's solution continued for more than a day, while reentry was sustained). Preincubation with and continued presence of N-acetyl-L-cysteine (NAC; 1-4

mM), an antioxidant, did not prevent the effects of diamide on APA (Figure 17) or the occurrence of reentry (2 out of 3 monolayers) as seen in Figure 18.

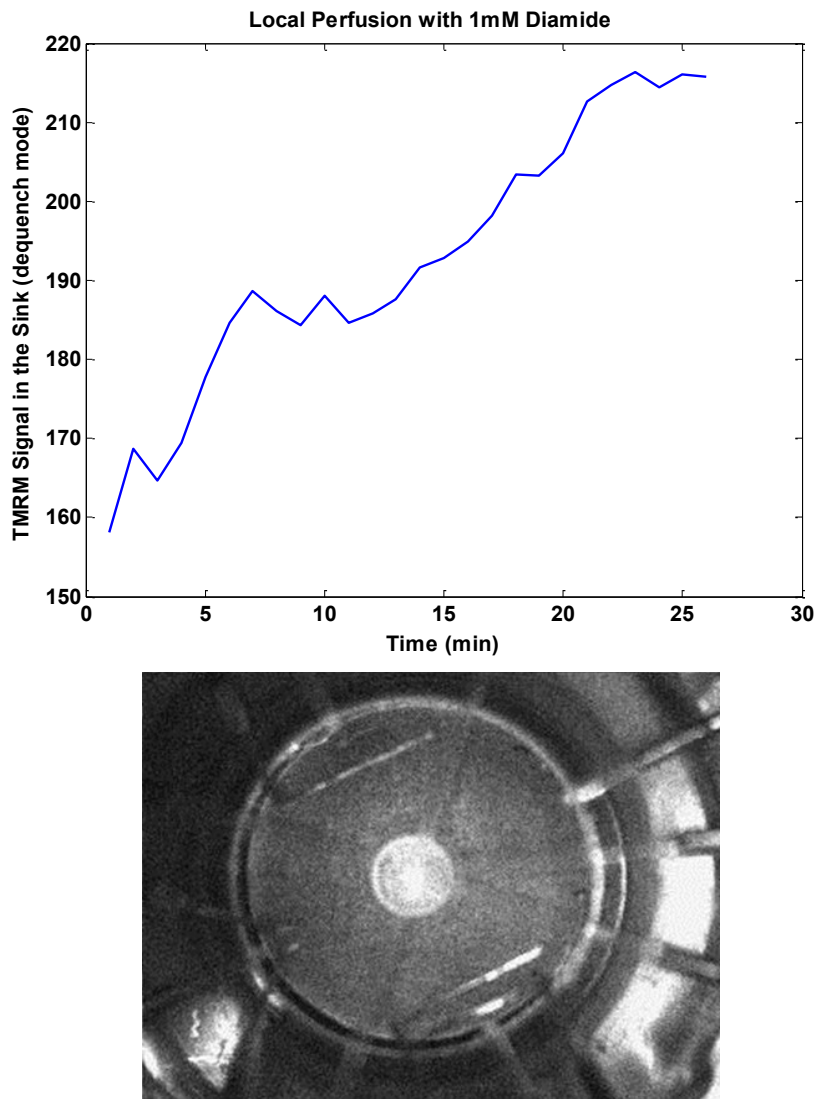
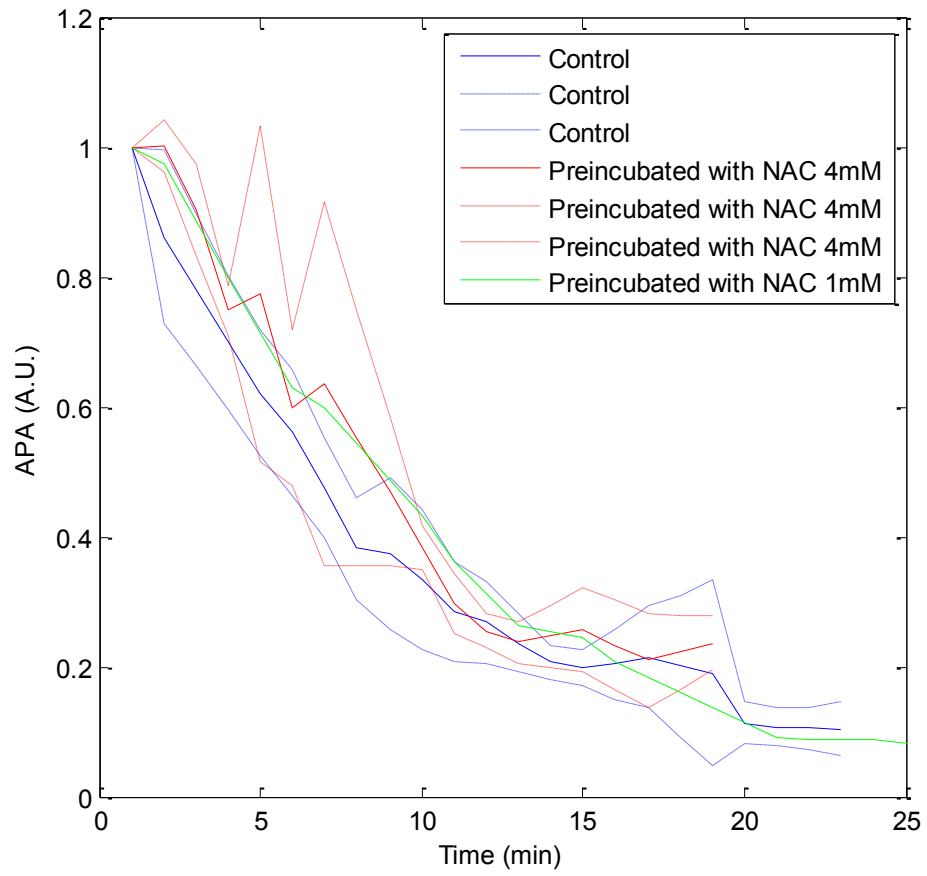


Figure 16 Effect of diamide on  $\Delta\Psi_m$ .

Upper: TMRM signal increases in the sink area as mitochondria become depolarized (dequench mode); Lower: An image of the TMRM loaded (2  $\mu$ M) monolayer after local perfusion with diamide (1 mM).





**Figure 17 Effect of diamide on APA.**

**Action potential amplitude decreased due to local perfusion with diamide (1mM).**

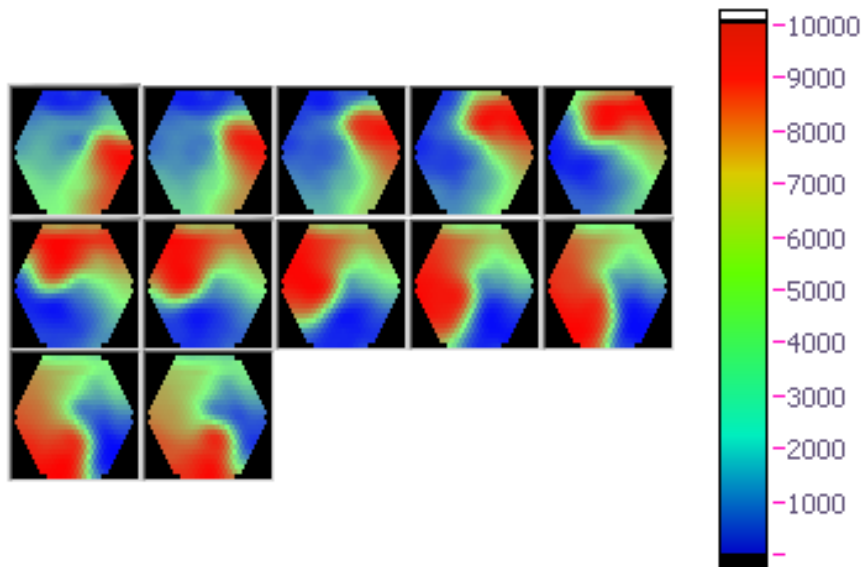


Figure 18 Reentry, 6 minutes after washout of diamide.

## 2.4 Conclusion

Previous experiments with intact hearts suggested that IR-induced mitochondrial depolarization is a major cause of IR-related arrhythmias<sup>28</sup>. For better observation of mitochondrial function and mapping of electrical activity, we needed a model less complex than the intact heart; thus, monolayers of cardiac myocytes were chosen as our experimental model.

Here, we demonstrated that the formation of a metabolic sink, resulting from regional mitochondrial depolarization, profoundly affects electrical activity in the tissue through mechanisms involving  $K_{ATP}$  channels. Induction of the metabolic sink was reversible and reentry occurred both during perfusion and washout of FCCP. The overall influence of

energetic collapse is to decrease APA and APD, decreasing wavelength and conduction velocity and introducing regions of very short refractory period that facilitate reentry. Electrophysiological heterogeneity or premature beats triggered at locations surrounding the metabolic sink resulted in spiral wave reentry in a sink size-dependent manner. Such premature beats might be triggered on the border zone of the ischemic area in intact hearts.

Induction of a metabolic sink by local perfusion with diamide led to inexcitability and occurrence of reentry, similar to the effects of diamide on intact perfused hearts<sup>35</sup>. While in whole heart experiments, when 4'-Cl-DZP was present, it prevented loss of  $\Delta\Psi_m$  and arrhythmias<sup>35</sup>, lack of recovery of excitability in our experiments suggests that PTP might be involved at this concentration of diamide, resulting in maintained inexcitability. This conforms with previous results from the experiments with isolated guinea pig cardiac myocytes in which when GSH/GSSG ratio was lowered to a threshold (50:1), PTP would be activated and  $\Delta\Psi_m$  depolarization would not be reversible<sup>10</sup>.

In a set of experiments, auranofin (10-100 nM) was used to depress the Thioredoxin reductase-dependent antioxidant system. Long-term perfusion with auranofin (>50 nM) lowered conduction velocity and excitability slightly; however, reentry was not seen. Excitability did not recover by washing auranofin out with normal media. Direct oxidative stress was also induced by locally perfusing the center of the monolayer with  $H_2O_2$ . Similar to the results of antioxidant depletion, recovery did not occur upon reperfusion.

Local perfusion of the center part of the monolayer with oligomycin at the concentration of 20  $\mu\text{M}$ , to block the ATP synthase, caused inexcitability which was not recovered by washout. Spiral wave reentry occurred both during perfusion and washout of oligomycin.

Blocking sarcolemmal  $\text{K}_{\text{ATP}}$  channels slowed the loss of APA and APD and lowered the chance of reentry in monolayers of cardiomyocytes. The effect of glibenclamide was even more evident at room temperature due to the much slower effect of FCCP. Our findings substantiate the involvement of  $\text{K}_{\text{ATP}}$  channels in electrical instability consequent to mitochondrial depolarization.

An increase in extracellular  $[\text{K}^+]$  during ischemia is known to depolarize the resting membrane potential and contribute to inexcitability and heterogeneity. We tested this idea by locally perfusing the center part of the monolayer with high- $[\text{K}^+]$  Tyrode's solution ( $[\text{K}^+] = 35 \text{ mM}$ ). Excitability and CV decreased, but the high- $[\text{K}^+]$ -perfused area did not become inexcitable. Reentry occurred upon washout when the monolayer was stimulated at 4 Hz.

For further examination of metabolic sink hypothesis, next we look at the effects of IR on mitochondrial function of the cardiac myocytes in a monolayer culture of NRVMs.

### 3 Metabolic Sinks Form during Ischemia/Reperfusion

#### 3.1 Introduction

In the previous chapter, we demonstrated the arrhythmogenic effects of metabolic sinks, formed by chemically-induced mitochondrial uncoupling, in monolayers of cardiomyocytes. We showed that perfusion of an area of the monolayer with mitochondrial uncoupler, FCCP, would cause slowing of CV, decrease in APA, shortening of APD and wavelength, and finally inexcitability of the region. Using glibenclamide to prevent  $K_{ATP}$  channels, we provided evidence that opening of  $K_{ATP}$  channels is a major factor in producing the aforementioned effects. It produces a large current of  $K^+$ ,  $I_{KATP}$ , which pulls the resting sarcolemmal membrane potential towards Nernst potential for  $K^+$ . Therefore, this area acts as a sink of current; i.e., stimulation current propagates through the monolayer and reaches the cells in this area but is nullified by outward current through  $I_{KATP}$ , failing to trigger an AP. Excitability and wave propagation would recover by washing FCCP out and reperfusing the sink with normal physiological solution. In many instances, these changes led to formation of reentrant waves.

In this chapter, we study the effect of IR on mitochondria of the cells in monolayers of cardiac myocytes to determine whether metabolic sinks form by inducing IR in our experimental model. Previously, de Diego *et al.*<sup>36</sup> used a coverslip-induced ischemia model<sup>37</sup> to study the electrophysiological consequences of IR in monolayers of cardiac myocytes. Placing a coverslip on a monolayer culture of cardiomyocytes leaves the cells with a thin film of media which well mimics the ischemic condition<sup>37</sup>. Active myocytes

consume the available oxygen and nutrients rapidly and produce metabolites which stay in the thin film at high concentrations. In the experiments done by, de Diego *et al.*, in response to induction of ischemia, AP amplitude (APA) and APD decreased, conduction velocity (CV) slowed, and wavelength (WL) shortened; moreover, arrhythmias formed in response to ischemia and reperfusion<sup>36</sup>.

To verify that these effects are due to ischemia and not the mechanical effects of placement of the coverslip, they showed that if the monolayers were cultured on a material permeable to oxygen and substrates, placement of a coverslip on the monolayer did not lead to the mentioned electrophysiological effects<sup>36</sup>. Also previously, using the same method, Pitts and Toombs, who first introduced this model, showed that changes in viability and contractility of the covered myocytes are not mechanical effects of coverslipping, but they are a result of the diffusion barrier formed by placement of the coverslip<sup>37</sup>.

Here, we use this experimental model to investigate the connection between the metabolic state and arrhythmogenicity in monolayers of NRVM's. Our findings show formation of regions with depolarized mitochondria with similar effects on AP as FCCP-induced metabolic sinks. We also find a strong correlation between failed or unstable recovery of mitochondrial function and occurrence of post-ischemic reentrant arrhythmias in monolayers of cardiac myocytes, supporting the metabolic sink hypothesis.

## **3.2 Methods**

### **3.2.1 NRVM Monolayers**

Neonatal rat ventricular myocytes (NRVM's) were isolated as described in the previous chapter.  $10^6$  cells were plated on each of circular cover glasses (D = 22mm) coated with fibronectin (25ug/ml) and supplemented with medium 199 (Invitrogen) containing 10% heat-inactivated bovine serum (Invitrogen). The media was changed daily. Experiments were performed on the 3rd to 5th day of culture.

### **3.2.2 Inducing Ischemia and Reperfusion**

All experiments started with superfusing the monolayer with Tyrode's solution consisting of (in mmol/l) 135 NaCl, 5.4 KCl, 1.8 CaCl<sub>2</sub>, 1 MgCl<sub>2</sub>, 0.33 NaH<sub>2</sub>PO<sub>4</sub>, 5 HEPES, and 5 glucose. The monolayer was paced by application of voltage pulses at 1 Hz using bipolar point or line electrodes. A 15 mm circular glass coverslip was placed on the center of the monolayer to reduce availability of Tyrode's solution and hence induce ischemic condition. Reperfusion was performed by lifting the coverslip after 1 hour of ischemia.

### 3.2.3 Recording $V_m$

To record the sarcolemmal membrane voltage and propagation of the excitation wave through the monolayer, we used an optical mapping technique, as described in the previous chapter. The dynamics of changes during ischemia were much slower than those during reperfusion; therefore in most of experiments, recordings were made every 1-5 minutes during ischemia versus every 10 seconds during reperfusion.

### 3.2.4 Measuring $\Delta\Psi_m$

To study the effect of IR on mitochondrial function, TMRM was used to record  $\Delta\Psi_m$ . For the dequench mode, cells were loaded with TMRM as described in the previous chapter (Page 14). For the linear mode, wherein TMRM fluorescence follows a distribution according to its Nernst potential<sup>34</sup>, monolayers were loaded with 50 or 100 nmol/l TMRM for 1 hour in the 37 °C incubator. In this mode, TMRM fluorescence is approximately linearly related to  $\Delta\Psi_m$ . Monolayers were then washed and put in normal Tyrode's solution in the heated (37 °C) chamber of an inverted microscope (Eclipse TE2000-E, Nikon). Excitation light of  $545 \pm 12$  nm was used and the fluorescence emission ( $605 \pm 35$  nm) was recorded with an EMCCD camera (Cascade II, Photometrics, AZ) using Micro-Manager (Vale Lab, UCSF, CA) or custom software developed in LabVIEW. Mitochondrial depolarization leads to loss of TMRM from the matrix and into the cytoplasm, which causes a decrease in the spatial dispersion of



TMRM fluorescence. Dispersion was calculated as the ratio of standard deviation to its mean. The data was analyzed using ImageJ and MATLAB.

### **3.3 Results**

#### **3.3.1 Depolarization and Repolarization of Mitochondrial Inner-Membrane during IR**

Initially, cells under normoxic conditions were paced at 1 Hz with voltage pulse stimulation applied at the edge of the monolayer. Mitochondria were stably polarized and  $\Delta\Psi_m$  was stable. After the coverglass was lowered on the central part of the monolayer,  $\Delta\Psi_m$  declined over time in the ischemic region. Figure 19 depicts the depolarization of mitochondrial membrane potential in the ischemic region, after 5 minutes (left) and 1 hour (right) of ischemia. Images were recorded using a 2x objective lens by fluorescence microscopy from TMRM-loaded cells in the dequench mode. A border zone of about 2 mm was observed between the edge of the coverslip and the ischemic zone, due to continued availability of oxygen diffusion into this region. Using the linear mode of TMRM at higher magnification (10x objective), individual myocyte mitochondrial networks can begin to be resolved (Figure 20A). Loss of  $\Delta\Psi_m$  in the central ischemic zone, but not the border zone, was evident after 1 hour of ischemia (Figure 20B). Reperfusion by coverslip removal initiated a general repolarization of  $\Delta\Psi_m$  in the formerly ischemic region (Figure 20C). Next, we examined the dynamics of  $\Delta\Psi_m$  loss and recovery at a higher spatial and temporal resolution.

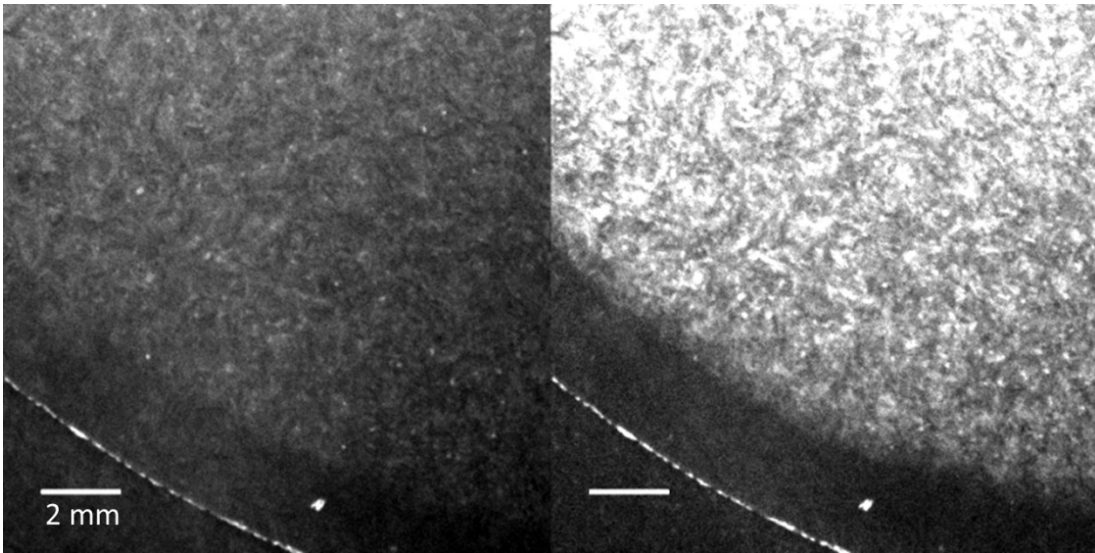


Figure 19  $\Delta\Psi_m$  at 5 minutes and 1 hour of ischemia.

$\Delta\Psi_m$  in the ischemic zone decreases during ischemia. Mitochondria in a border zone of approximately 2 mm stay polarized (TMRM 2  $\mu$ M, dequench mode).

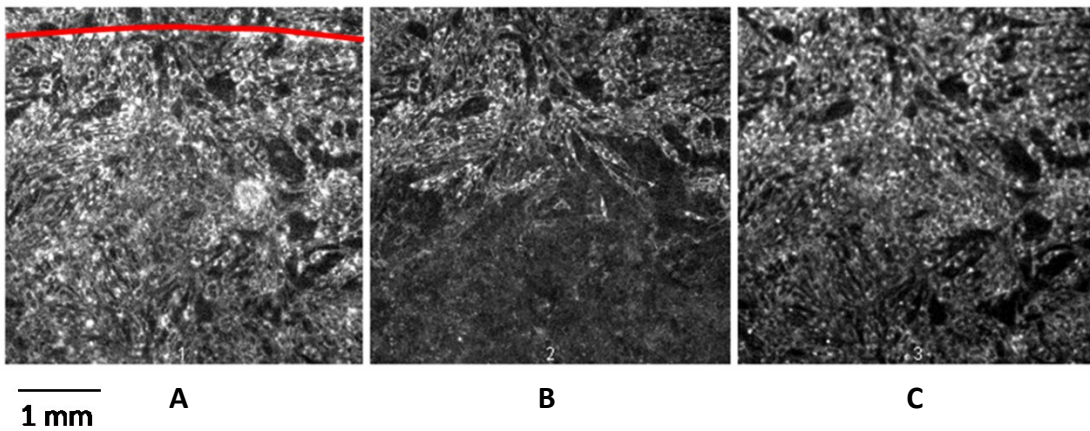


Figure 20 Effect of 1 hour ischemia on the  $\Delta\Psi_m$ .

A: Start of ischemia; red line shows the edge of the coverslip; the small area on top of the red line is not covered. B: Start of reperfusion. C: After 2 hours of reperfusion.

### 3.3.1.1 $\Delta\Psi_m$ during Ischemia

In the ischemic region,  $\Delta\Psi_m$  was lost in two phases: an initial slow and partial phase and a rapid global decline. During the initial phase, individual clusters of mitochondria became depolarized (Figure 21). Cells in the ischemic region stopped contracting approximately 6 minutes after coverslip placement.

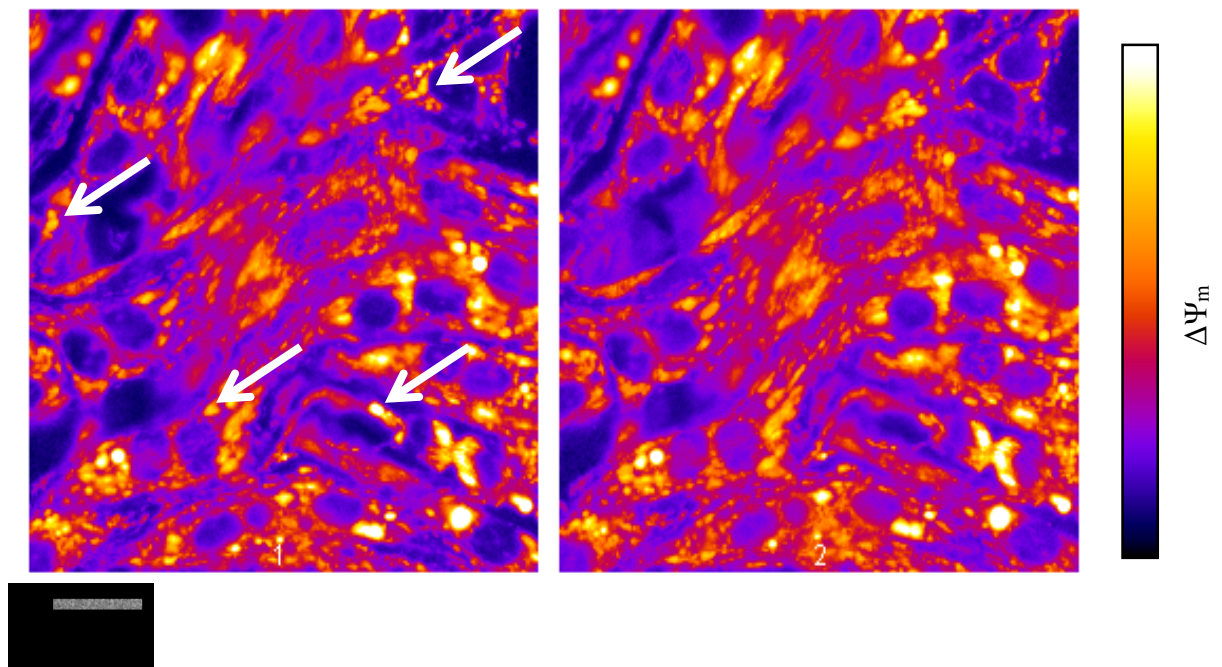
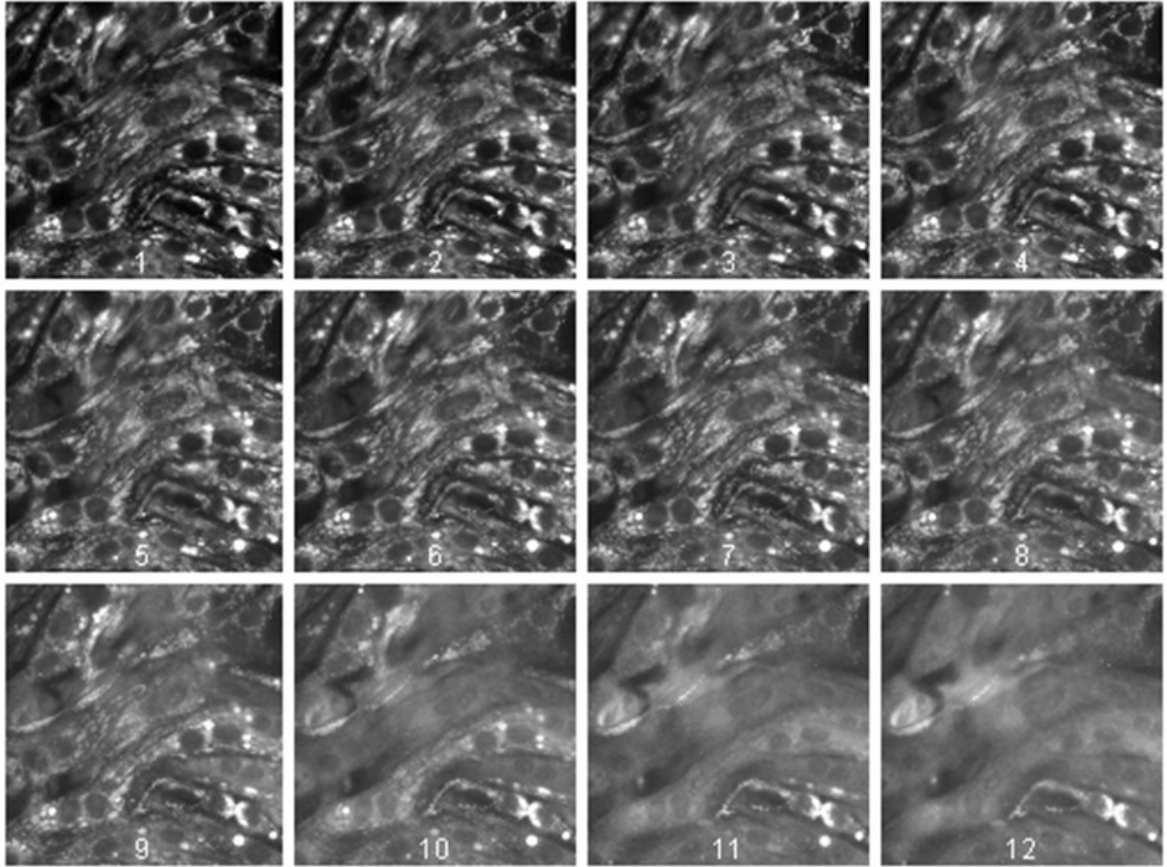


Figure 21 First phase of mitochondrial depolarization due to ischemia.

During the first phase of  $\Delta\Psi_m$  depolarization, individual clusters of mitochondria become depolarized. These images are from the myocytes at the central region of the monolayer at 10 (left) and 20 minutes (right) of ischemia. Arrows show examples of clusters of mitochondria that became depolarized during the first phase of  $\Delta\Psi_m$  loss. Bipolar stimulation at 2 Hz. 40x objective lens; fluorescence intensity scaled by color from black through white using a lookup table.

During the second phase, which started after  $32.9 \pm 8.6$  minutes of ischemia ( $N = 9$ ), the mitochondrial network of the myocytes rapidly became depolarized and cells underwent contracture (Figure 22). The dynamics of changes in  $\Delta\Psi_m$  can be studied by plotting the dispersion of TMRM signal. Figure 24 shows the decrease in dispersion (i.e.,  $\Delta\Psi_m$  depolarization) during these two phases over 60 minutes of ischemia for one monolayer. This can be explained by the hypothesis of criticality which was described in the first chapter. When enough number of mitochondria became depolarized and the stress applied on the cardiomyocytes in the ischemic region reached a critical value, this causes instability of the whole mitochondrial network of the cells which can propagate to the neighboring cardiomyocytes.

Based on our recordings from a larger area of the monolayer, loss of  $\Delta\Psi_m$  started from the center and extended outwards (Figure 23).



**Figure 22** Effect of long-term ischemia on  $\Delta\Psi_m$ .

Cells in the center of the monolayer underwent 1 hour of ischemia (5-minute interval, TMRM 100nM, 40X,  $150\ \mu\text{m} \times 150\ \mu\text{m}$ ).  $\Delta\Psi_m$  is lost in two phases: a slow and partial phase (images 1-8) and then a rapid global phase (images 9-12).

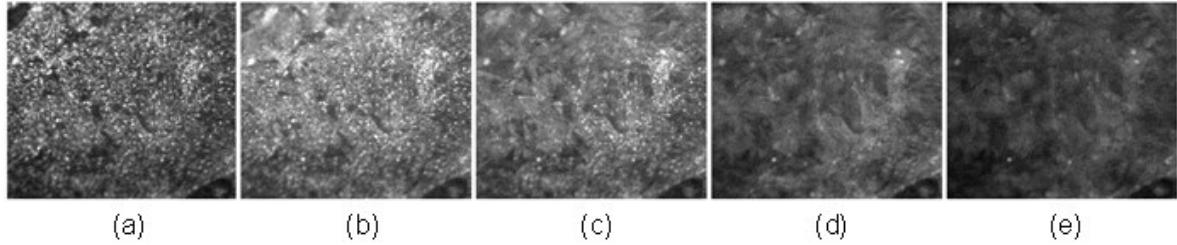


**Figure 23 Wave of depolarization of  $\Delta\Psi_m$  during ischemia.**

**Mitochondria lose  $\Delta\Psi_m$  during ischemia in a wave propagating through the monolayer from the center towards the edge of the coverslip.**

During the coverslip-induced ischemia protocol, mitochondria in the uncovered area and the border zone were stable, apart from occasional flickering of a few individual mitochondria on the border zone. Observing the monolayer during a long period of ischemia showed that the mitochondria in the border zone stayed polarized even after 17 hours of ischemia followed by subsequent reperfusion.

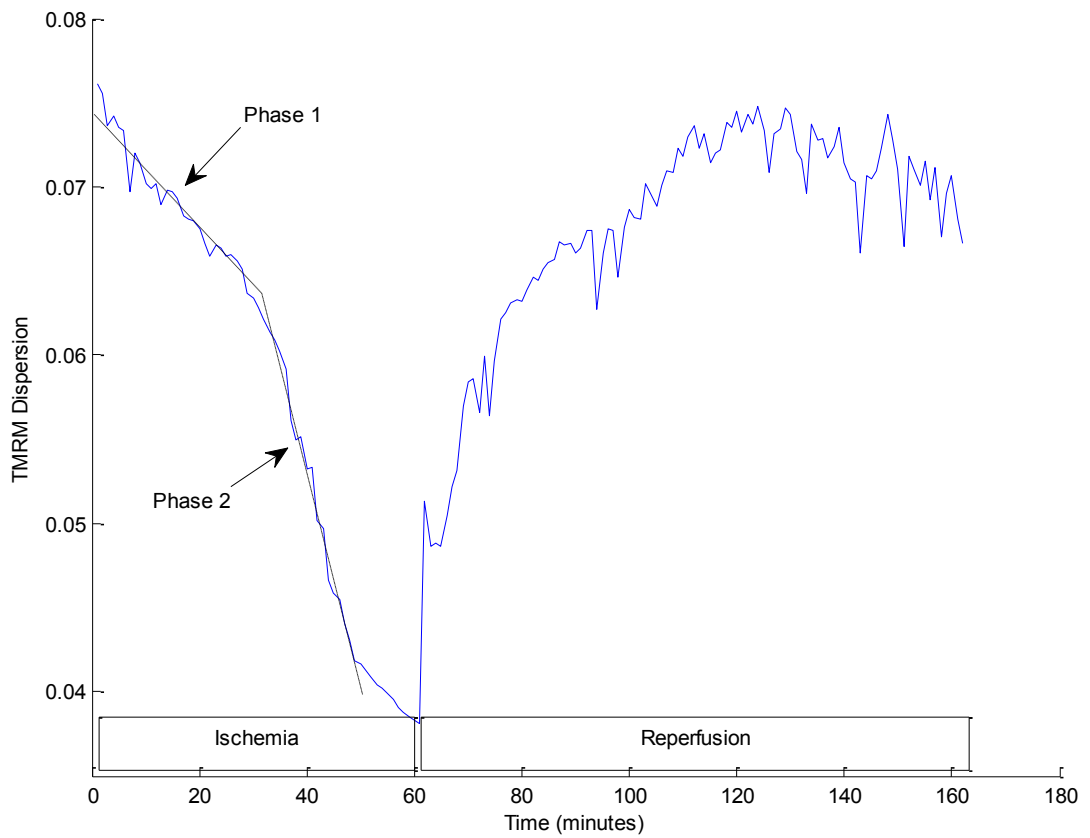


**Figure 24 Change of  $\Delta\Psi_m$  during ischemia and reperfusion.**

**Changes in distribution of TMRM during IR can be measured as changes in spatial fluorescence dispersion. During Ischemia, TMRM exits the mitochondria and enters the cytoplasm leading to a decrease in dispersion. Upon reperfusion, mitochondria gradually rebuild  $\Delta\Psi_m$  as indicated by an increase in TMRM dispersion as the dye redistributes back into the mitochondrial matrix.  $\Delta\Psi_m$  instability limits the overall recovery rate of mitochondrial membrane potential.**

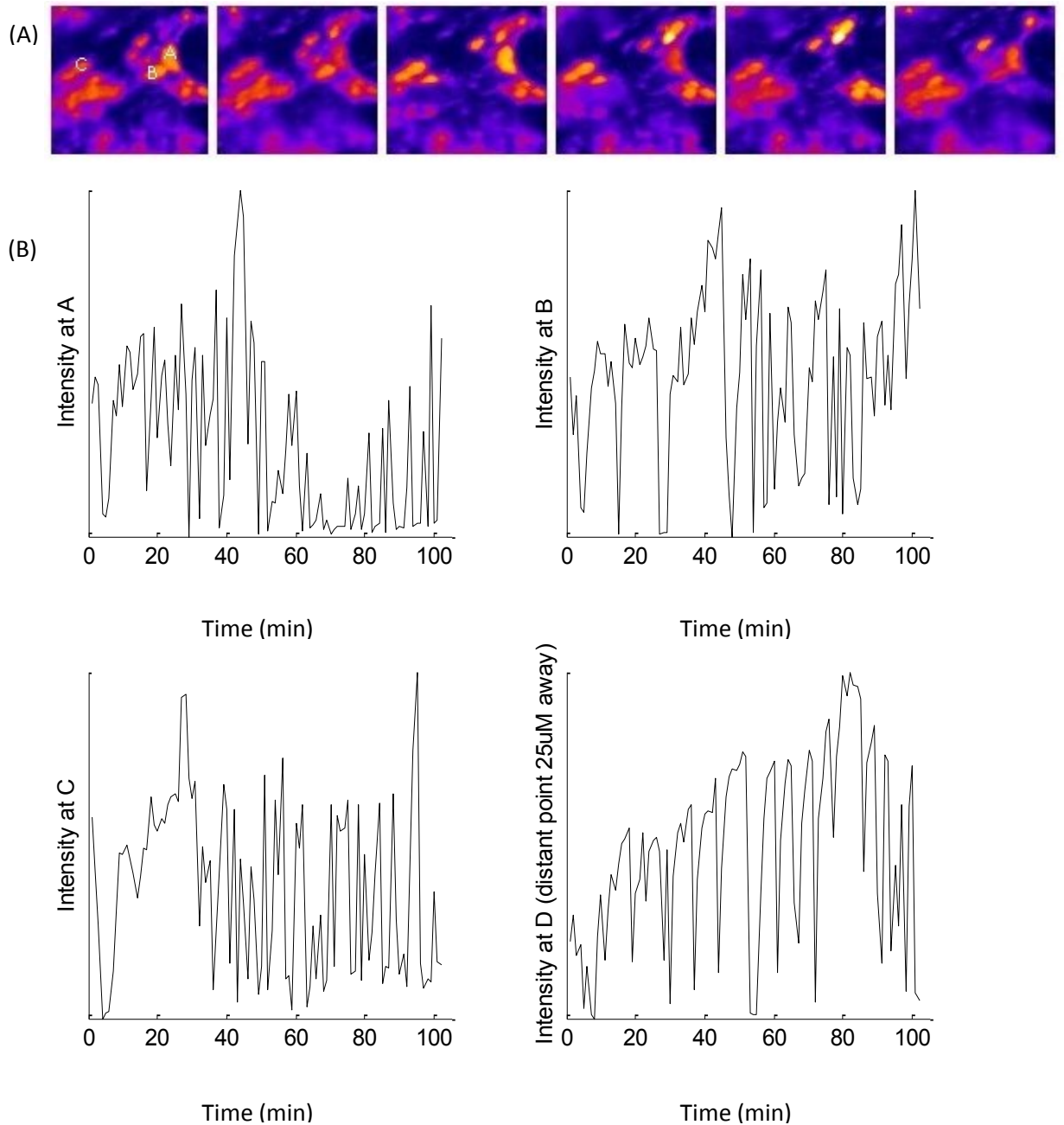


**Figure 25 Oscillation of  $\Delta\Psi_m$  upon reperfusion.**

**A:** A part of a cell in the monolayer, cropped from the  $40\times$  images. Interval 1 minute; minutes 50-55 of reperfusion. Dimensions  $25\mu\text{m} \times 25\mu\text{m}$ . **B:**  $\Delta\Psi_m$  instability illustrated by plotting the intensity of TMRM signals at points A, B, C (from the same cell; shown on first slide of part (A)), and D (from a separate myocyte  $25\mu\text{m}$  away).



### 3.3.1.2 $\Delta\Psi_m$ during Reperfusion

Reperfusion during the first phase of mitochondrial depolarization (up to 30 minutes of ischemia) resulted in stable recovery of  $\Delta\Psi_m$ ; however, extending the ischemic period to 1 hour of ischemia resulted in an unstable recovery of  $\Delta\Psi_m$  following reperfusion (Figure 24). Oscillations (freq  $<20$  mHz) of  $\Delta\Psi_m$ , evident as random flickering of separate clusters of mitochondria (Figure 25) were observed over the field of view in the post-ischemic zone ( $150\ \mu\text{m} \times 150\ \mu\text{m}$ ). Early after reperfusion, the adjacent clusters showed highly synchronized oscillations within individual myocytes, consistent with RIRR as a coupling factor; later in the reperfusion period the correlation between  $\Delta\Psi_m$  oscillations in adjacent mitochondrial clusters declined (Figure 26).

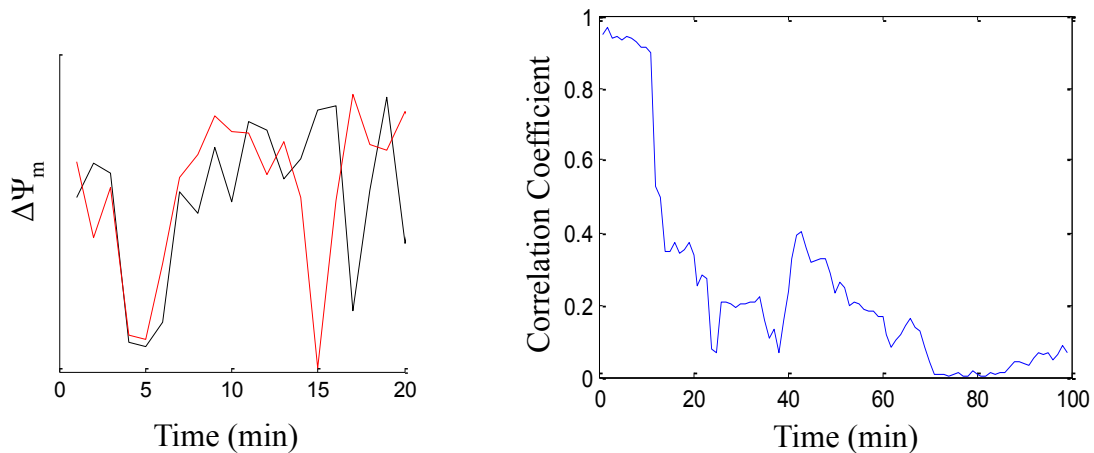


**Figure 26 Oscillations of adjacent clusters are synchronized during early reperfusion.**

**Left:**  $\Delta\Psi_m$  shown by intensity of TMRM signal at two adjacent clusters (A and B from the previous figure) during the first 20 minutes of reperfusion. **Right:** Correlation coefficient of  $\Delta\Psi_m$  changes in the adjacent clusters decreases through time.

$\Delta\Psi_m$  oscillations after reperfusion were gradually sustained for the whole period of recording (up to 120 minutes). However, in some cases, the mitochondrial network of an individual myocyte or a few myocytes depolarized abruptly. This depolarization affected the neighboring myocytes and a wave of depolarization propagated through the monolayer. This type of depolarization, which was irreversible, occurred with variable onset after reperfusion. Such an event could start 2 hours after the onset of reperfusion, or as shown in the dispersion plot in Figure 31 – black line, it could start much earlier during reperfusion.

Notably, in some experiments, the reperfusion-induced mitochondrial instability was observed to spread beyond the post-ischemic zone; the border zone and normoxic regions of the monolayer underwent sporadic and dispersed loss of  $\Delta\Psi_m$ , even though they had not been affected during ischemia. This suggests that toxic metabolites can diffuse out of the ischemic zone to destabilize mitochondria in otherwise healthy cells.

### **3.3.2 IR-Induced Arrhythmias**

With an understanding of the mitochondrial responses to ischemia and reperfusion in the monolayer, we next investigated the effects of ischemia/reperfusion on electrical excitability and arrhythmias. Under normoxic control conditions, the excitation wave, recorded by optical mapping, propagated through the monolayer uniformly with  $CV = 15.5 \pm 6.1$  cm/s ( $N = 10$ ), evoking APs with  $APD = 138 \pm 54$  ms ( $N=15$ ). After placing the coverslip over the center part of the monolayer, the APA and APD decreased (5

minutes after the onset of ischemia:  $APA = 77 \pm 25 \%$ ,  $APD_{50} = 57.9 \pm 30.8 \%$  of initial values, the conduction velocity (CV) slowed (to  $8.3 \pm 4.4$  cm/s). Therefore, the wavelength, WL, shortened in the ischemic area over time. After  $15.4 \pm 5.4$  minutes ( $N = 13$ ), the area under the coverslip became completely inexcitable (Figure 27). At this time, the activation wave passed around the ischemic area, exciting only the cells in the outer region and the border zone. Reentry was not a typical event during ischemia; although in 3 out of 18 monolayers, when the monolayer was paced at 3 Hz, a heterogeneous decrease in excitability beneath the coverglass caused a unidirectional block and led to reentry.

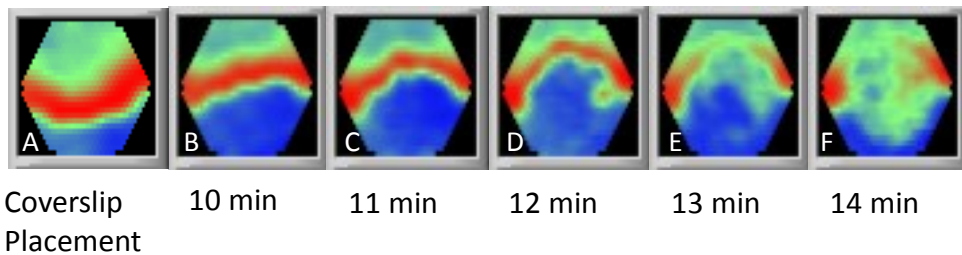


**Figure 27** Coverslip-induced ischemia affects the propagation of the excitation wave.

Excitability recovered shortly after reperfusion, however not homogeneously (Figure 28). The recovery started  $1.1 \pm 0.6$  minutes ( $N = 12$ ) after the onset of reperfusion, with formation of several slow-propagating stray wavelets in the ischemic zone. Due to low CV and short WL in this region, this phase was soon (ranging from a few seconds up to 3

minutes) replaced by micro-reentries and fibrillatory activity. This evolved into sustained reentry anchored on the boundary between the border zone and ischemic zone, in 5 out of 8 monolayers. The anchor of reentry either remained at the same point or migrated to other points on the boundary. Reentry also occurred in 5 out of 7 monolayers, if the monolayer was reperfused after a short ischemia of only  $19.7 \pm 5.3$  minutes (ranging 11-30 minutes), while being stimulated at 3 Hz.

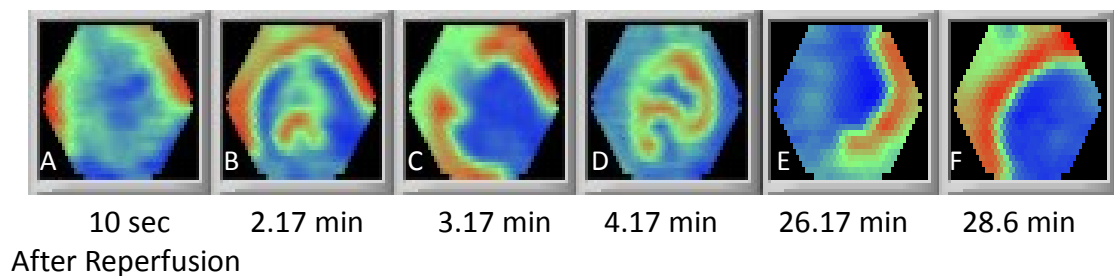


**Figure 28 Electrical propagation during reperfusion.**

**A:** The excitation wave passes around the reperfused area; **B:** After a short time, wavelets form in the reperfused area; **C:** Formation of two reentrant waves with rotors located on the boundary of border zone and reperfused zone; **D:** Three reentrant waves underlying fibrillatory activity; **E:** Small reentrant waves coalesce and form a single reentrant spiral wave; **F:** After a few minutes the reentrant wave dies out and nearly normal propagation is seen. CV in the reperfused area, however remained slow through the end of this experiment (38 minutes of reperfusion).

### 3.3.3 Effect of 4'-Cl-DZP on mitochondrial instability

As explained in the introduction, the peripheral benzodiazepine receptor ligands 4'-Cl-DZP or PK-11195 were shown to stabilize stressed mitochondria and prevent depolarization and oscillation of  $\Delta\Psi_m$  in isolated adult cardiomyocytes. Additionally, 4'-Cl-DZP was shown to be effective in preventing IR-induced or oxidative stress-induced cardiac dysfunction in whole heart experiments, while preserving mitochondrial membrane potential<sup>28</sup>. These effects were interpreted to suggest that IMAC was the main target involved in mitochondrial RIRR. Here, we examine the effects of blocking IMAC using 4'-Cl-DZP on IR-induced mitochondrial oscillations and arrhythmogenicity in NRVM monolayers.

The presence of 4'-Cl-DZP did not affect the loss of  $\Delta\Psi_m$  during ischemia in our experiments (phase 2 starting at  $37.5 \pm 10.6$  minutes; see Figure 29). However, when 4'-Cl-DZP was present in the media at the concentration of 16  $\mu\text{M}$ ,  $\Delta\Psi_m$  stably recovered upon reperfusion. Only a few clusters showed oscillations and these oscillations were very sparse (Figure 30). Higher concentrations of 4'-Cl-DZP (64  $\mu\text{M}$ ) did not stabilize mitochondrial energetics after reperfusion.

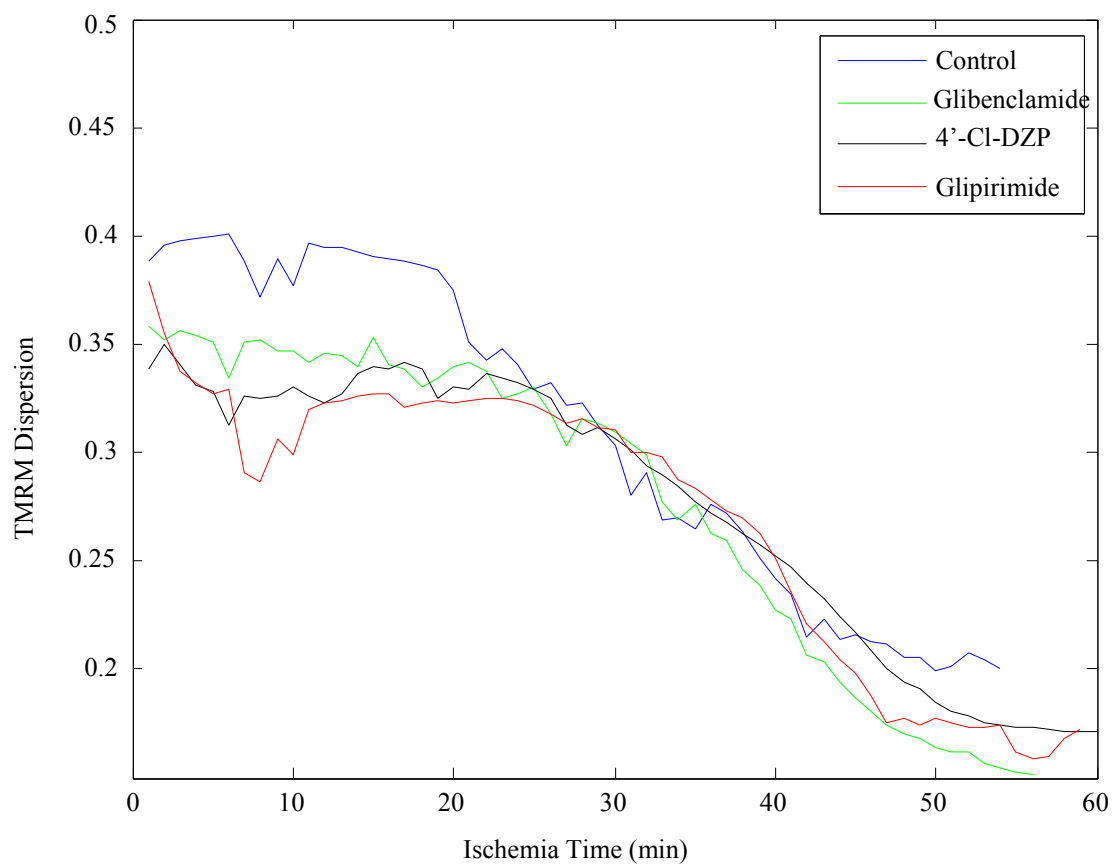


**Figure 29** Effect of different chemicals on ischemia-induced mitochondrial depolarization.

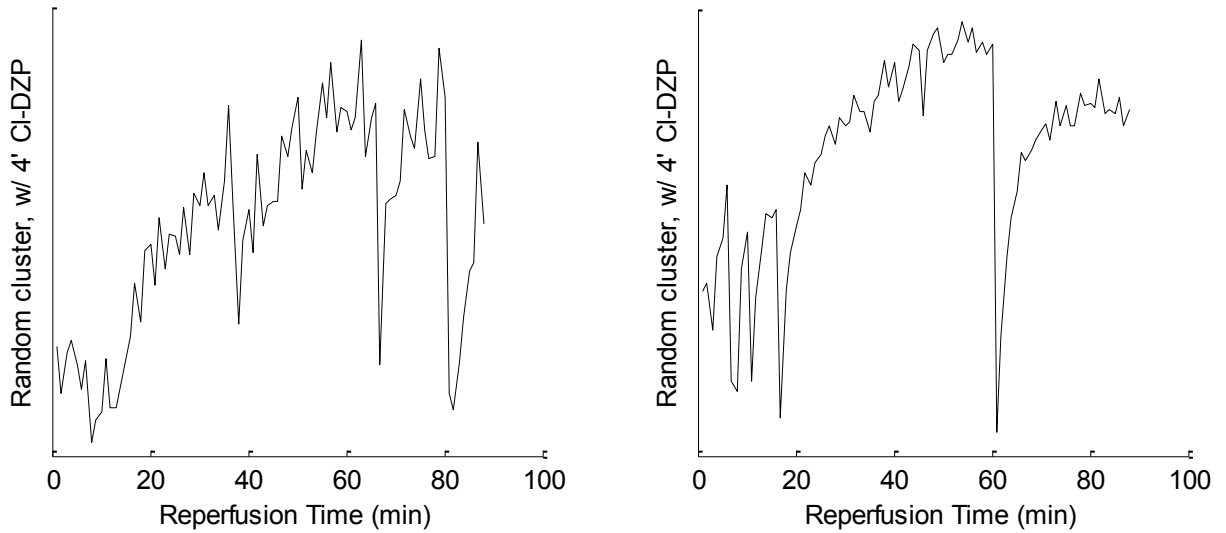


**Figure 30 4'-Cl-DZP stabilizes the mitochondria.**

**Sparse oscillations were seen in very few mitochondrial clusters (time course shown for two such clusters in the panels) in an image field of  $150\ \mu\text{m} \times 150\ \mu\text{m}$  in the reperfused zone of the monolayer after 1-hour ischemia when 4'-Cl-DZP was present in the media at  $16\ \mu\text{M}$ .**

We also tested for the involvement of PTP in IR-induced mitochondrial oscillations in separate experiments. The inhibitor of PTP, CsA, was used at a  $1\ \mu\text{M}$  concentration. The presence of CsA over the entire ischemia/reperfusion protocol did not prevent ischemia-induced loss of  $\Delta\Psi_m$ , nor did it suppress oscillations of  $\Delta\Psi_m$  after reperfusion, refuting a causal role for PTP in reperfusion-induced mitochondrial oscillations. On the other hand, the loss of  $\Delta\Psi_m$  at late reperfusion was prevented by CsA (as shown in Figure 31), suggesting a role for PTP in mitochondrial loss during late reperfusion. These findings are consistent with previous work demonstrating that there is sequential activation of the IMAC (4'-Cl-DZP-sensitive) and PTP (CsA-sensitive) upon oxidative stress<sup>10</sup>. Also

consistent with the present findings, PTP is shown to open by 15 minutes after the onset of reperfusion in experiments on isolated rat hearts<sup>38</sup>.

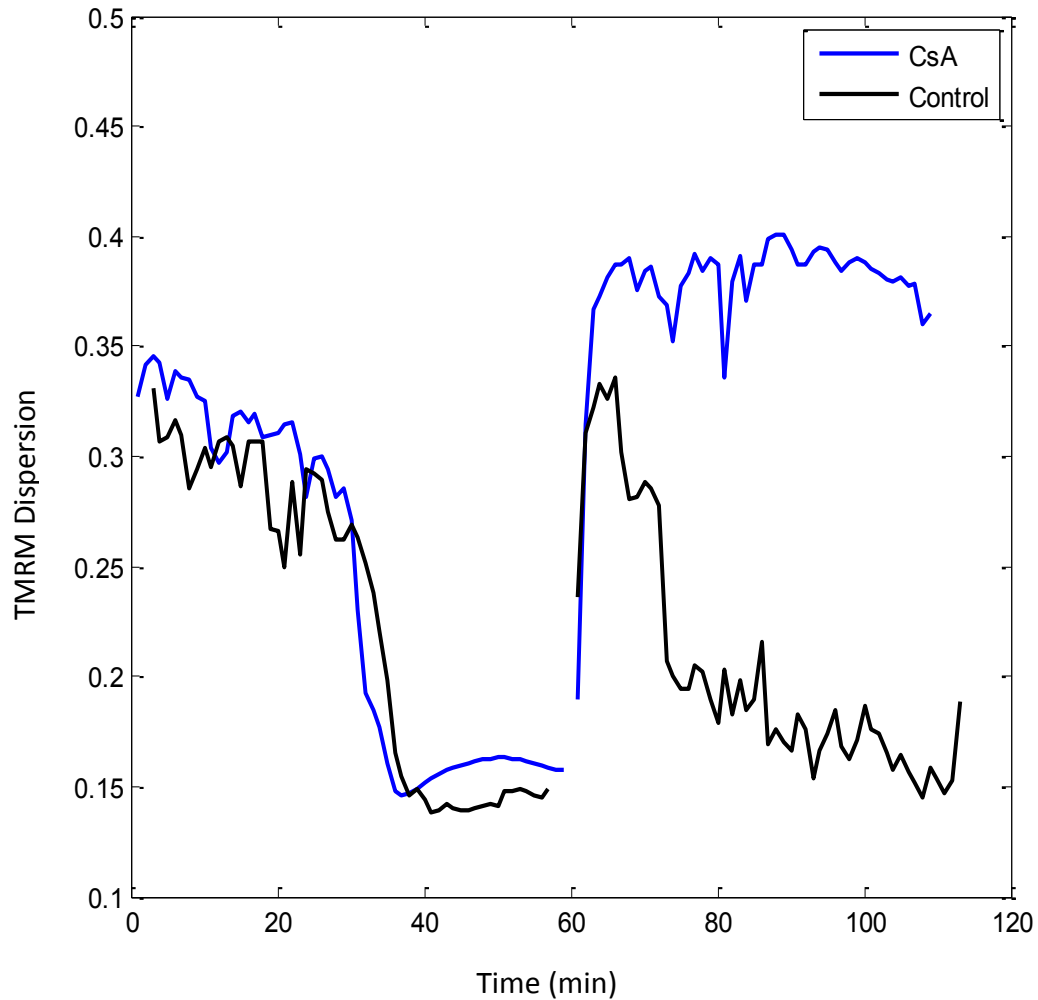


**Figure 31 PTP involvement in large-scale reperfusion-induced mitochondrial  $\Delta\Psi_m$  loss.**

**While not able to prevent oscillations, CsA can protect mitochondria from total depolarization. Both monolayers are from the same cell preparation; CsA was applied at 1  $\mu$ M. Horizontal axis shows the time in minutes from the onset of ischemia. Reperfusion starts at 60 minutes.**



### **3.3.4 Effect of 4'-Cl-DZP on reentry induced by reperfusion**

While 4'-Cl-DZP was shown to blunt APD shortening in intact perfused hearts during ischemia<sup>28</sup>, in our experiments, 4'-Cl-DZP accelerated the inexcitability induced by coverslip-induced ischemia in the NRVM monolayers. Recovery of excitability upon reperfusion was also somewhat delayed. For several minutes after the initial recovery of AP generation, the monolayer did not respond to the stimulation pulses in a 1:1 fashion. However, by 10-20 minutes after the reperfusion started, the monolayer became normally excitable.

As shown in Figure 32, while 4'-Cl-DZP treatment slowed recovery after ischemia, it prevented early reperfusion-induced reentry and facilitated a near complete recovery of APD to the preischemic values within 2-4 minutes. Spontaneous activity elicited on the border zone was also suppressed, occurring only in 1 out of 5 monolayers, with this singular event leading to reentry 20 minutes after the onset of reperfusion (late reperfusion arrhythmia).

### **3.3.5 Effect of Blocking $K_{ATP}$ channels during IR**

Blocking K-ATP channels did not affect the dynamics of mitochondrial depolarization during ischemia (Figure 29). Unexpectedly, when glibenclamide or glimepiride (another blocker of  $K_{ATP}$  channels) were used in our experiments, mitochondrial instability increased: the frequency of mitochondrial oscillations increased (compare Figure 33 with

the first 25 minutes of  $\Delta\Psi_m$  diagrams in Figure 25B). This might be due to the known nonspecific mitochondrial uncoupling effect of glibenclamide<sup>39</sup>, but a detrimental effect was not observed in the FCCP experiments described earlier. Also, arrhythmogenicity was not affected when glibenclamide was present in the media at 10  $\mu\text{M}$  and reentry occurred in 7 out of 8 monolayers. This negative effect of  $\text{K}_{\text{ATP}}$  channel inhibition during ischemia/reperfusion thus differed from the anti-arrhythmic effect of glibenclamide observed during chemical uncoupling of mitochondria. This is likely due to the fact that ischemia/reperfusion induces a much more complex set of cellular changes that cannot be reversed by inhibition of a single ion channel target. Unlike the agents that prevented mitochondrial depolarization (e.g., 4'-Cl-DZP),  $\text{K}_{\text{ATP}}$  channel inhibition would not be expected to prevent the global defects in energy supply and ROS imbalance that accompanies ischemia. Moreover, as these  $\text{K}_{\text{ATP}}$  channel inhibitors are not specific to sarcolemmal  $\text{K}_{\text{ATP}}$  channels, the detrimental actions of these compounds could be the results of blocking mitochondrial  $\text{K}_{\text{ATP}}$  channels. Mitochondrial  $\text{K}_{\text{ATP}}$  channels were shown previously to be critical in ischemic preconditioning<sup>40-42</sup>; hence blocking them might prevent their protective effects.

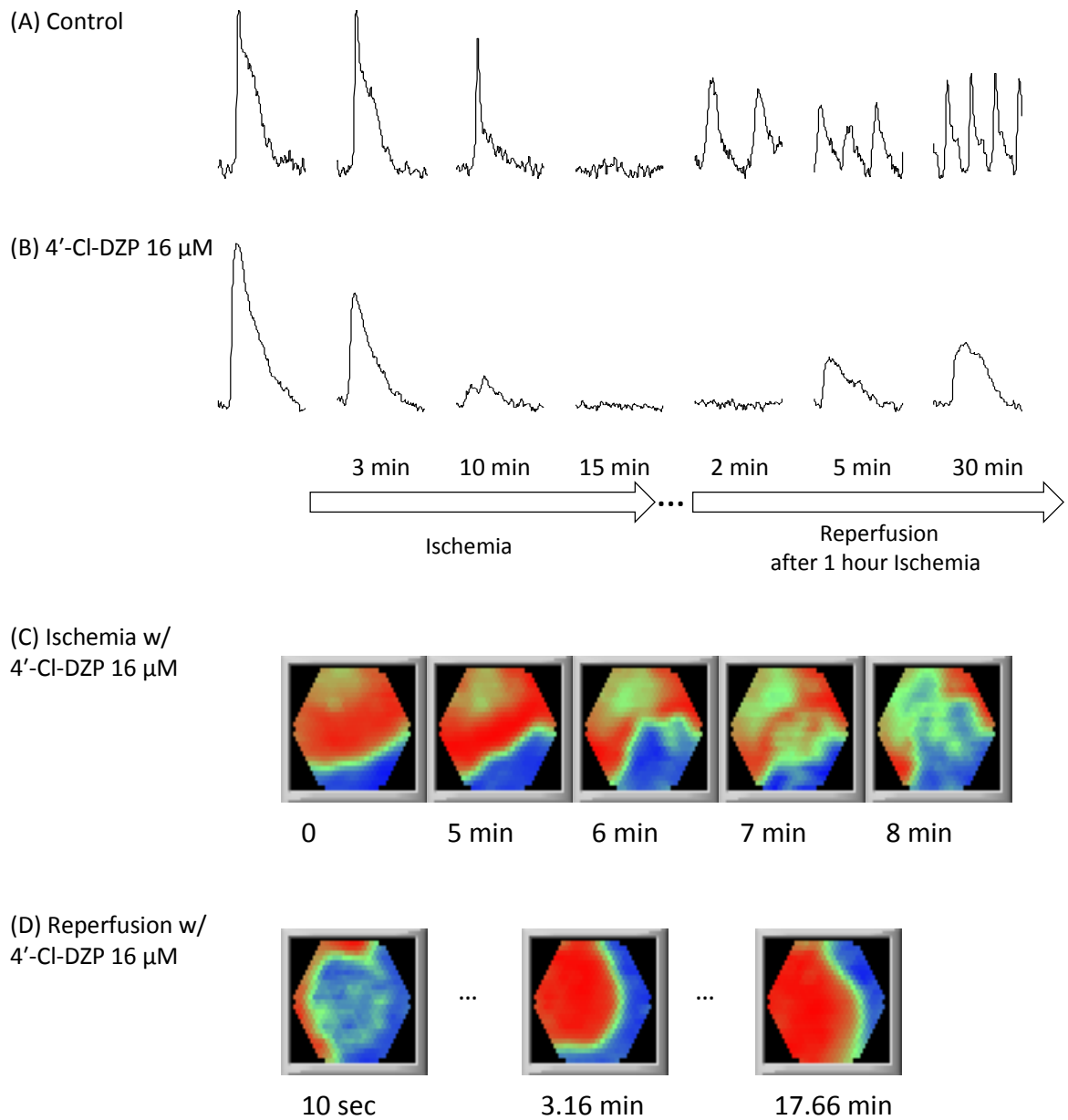


**Figure 32 4'-Cl-DZP stabilizes electrical activity.**

**A: Changes in optical action potential amplitude and duration during IR. B: 4'-Cl-DZP prevents APD shortening, but does not affect APA change. C: Ischemia renders the monolayer inexcitable with/without 4'-Cl-DZP. D: Early after reperfusion, reentry was never seen in the presence of 4'-Cl-DZP at 16  $\mu$ M, while in control monolayers, sustained reentry was seen frequently.**

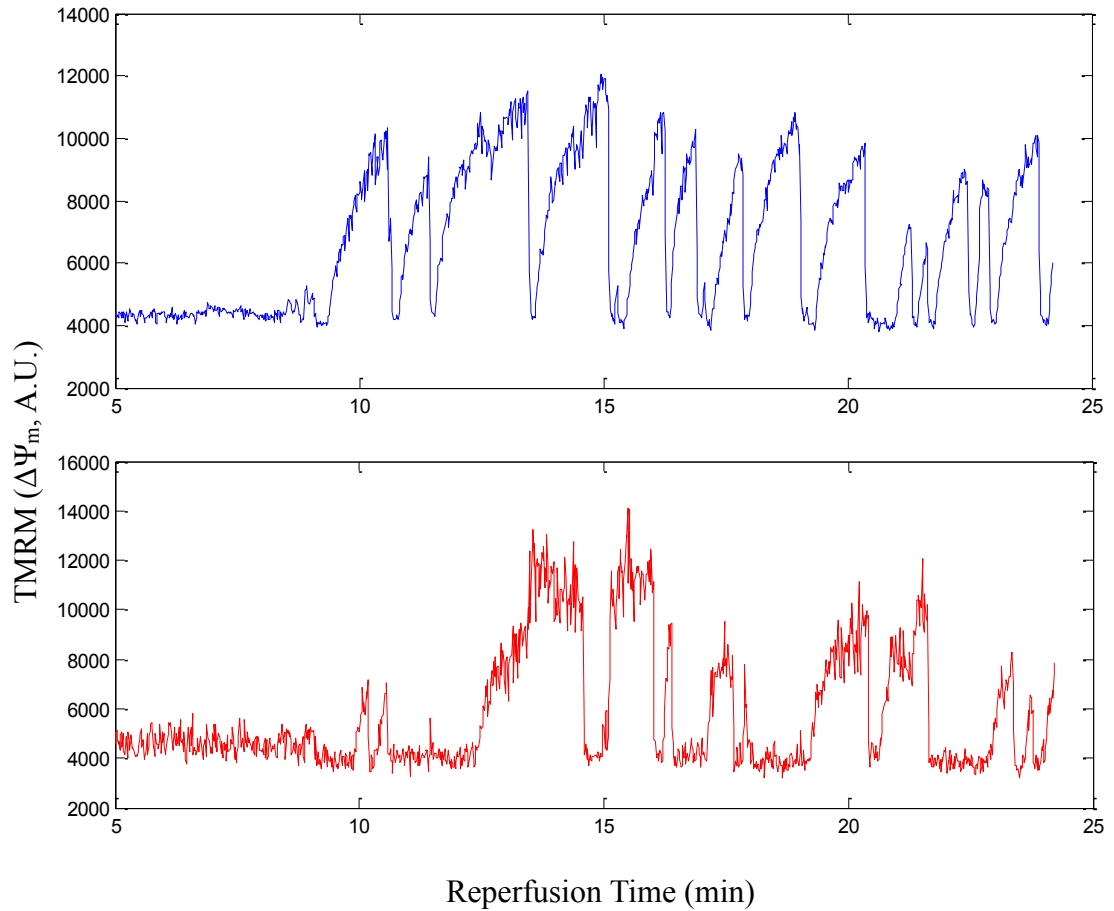


**Figure 33 Effect of  $K_{ATP}$  inhibition on mitochondrial instability.**

**Glimepiride at the concentration of 10  $\mu\text{M}$  was present in the media. Mitochondrial flickering is increased compare to control.**

### **3.4 Conclusion**

Available evidence suggests a correlation between mitochondrial dysfunction and arrhythmogenicity in hearts subjected to ischemia/reperfusion. In guinea pig hearts,

reperfusion after 30 minutes of global ischemia evokes reentrant arrhythmias, and treatment with a compound that prevents or reverses RIRR-mediated mitochondrial depolarization (4'-Cl-DZP) eliminates post-ischemic VF and improves AP recovery<sup>28</sup>. More recently, direct evidence was reported that significant spatiotemporal heterogeneity of  $\Delta\Psi_m$  is present during ischemia/reperfusion in isolated hearts<sup>6,7</sup>. In isolated cardiac myocytes, metabolic or oxidative stress, induced by substrate deprivation, glutathione depletion, or localized laser flash, leads to instability and oscillations of  $\Delta\Psi_m$ <sup>10,12,43</sup>. These observations led to the proposal that mitochondrial instability is a major factor contributing to arrhythmic events associated with IR. Metabolic sinks of current due to opening of sarcolemmal  $K_{ATP}$  channels were proposed to underlie the heterogeneity in APD, refractory period, and excitability, setting the stage for reentry.

Here, we demonstrate that mitochondrial instability is prevalent in an *in vitro* model of ischemia/reperfusion in monolayers of NRVMs and that reperfusion arrhythmias are correlated with mitochondrial dysfunction. Stabilization of  $\Delta\Psi_m$  prevents reentry on reperfusion and stabilizes the cardiac action potential. The development of this platform for studying IR at the cellular level allowed us, for the first time, to examine the time course of  $\Delta\Psi_m$  loss and recovery in detail while studying the concurrent electrophysiological changes in parallel. Importantly, reperfusion markedly destabilizes and desynchronizes the mitochondrial network of the cells in the NRVM monolayer; this instability can also spread to border zone and outer regions. Mitochondrial oscillation between the energized and de-energized states reveals that spatiotemporal heterogeneity of energetics, as well as electrical excitability, spans from the subcellular to the syncytial level. Our results showed that 4'-Cl-DZP, but not CsA, could prevent mitochondrial

destabilization and facilitate AP recovery upon reperfusion, preventing post-ischemic arrhythmias. The results support the idea that mitochondrial instability is a major factor in occurrence of IR-related arrhythmias.

## 4 Discussion and Conclusions

Heterogeneous instability of APs and corresponding changes in the dispersion of repolarization can cause arrhythmias<sup>44</sup> in intact myocardium. In isolated cardiac myocytes subjected to metabolic or oxidative stress,  $I_{KATP}$  was observed to oscillate, inducing action potential (AP) alterations<sup>8,45</sup>. Inhibition of IMAC with 4'-Cl-DZP, an antagonist of mitochondrial benzodiazepine receptor (mBzR), inhibited oscillations of both  $\Delta\Psi_m$  and APD in individual cardiomyocytes<sup>28</sup> and prevented arrhythmias in whole hearts at the onset of reperfusion<sup>28,46-48</sup>, adding to the evidence for a link between mitochondrial function and arrhythmias during IR. Previously, the concept of metabolic sinks was introduced as clusters of cells with depolarized or unstable mitochondria, formed due to IR-induced metabolic stress, which could alter the propagation of electrical excitation and potentially lead to reentry<sup>28</sup>.

Mitochondrial  $\Delta\Psi_m$  depolarization potentiates  $K_{ATP}$  channel opening because the resulting uncoupling of oxidative phosphorylation leads to the reversal of the mitochondrial ATP synthase, accelerating the depletion of intracellular ATP<sup>15</sup>. Sarcolemmal  $K_{ATP}$  channels are activated by a decrease in cytosolic ATP/ADP ratio and mediate a weakly inwardly rectifying background  $K^+$  current<sup>30,31</sup>. Increased background  $K^+$  conductance through  $K_{ATP}$  channels pulls the resting membrane potential close to the equilibrium potential for  $K^+$  ( $E_K$ ). After 10 minutes of ischemia, resting membrane potential is, in fact, equal to  $E_K$ <sup>49</sup>.  $K_{ATP}$  current activation accounts for most of the AP shortening during the early phase of ischemia, as evidenced by the ability of  $K_{ATP}$  channel inhibitors such as glibenclamide to prevent shortening of the APD over the first

10 minutes of ischemia<sup>28</sup>. Concomitant with AP shortening, there is a monotonic decrease in APA and upstroke velocity during the first 10 minutes of ischemia, which can be partially prevented by glibenclamide treatment<sup>28</sup>, suggesting that  $K_{ATP}$  channels may contribute to both the AP shortening and early conduction slowing in the ischemic heart. Interestingly,  $K_{ATP}$  antagonists can also prevent ventricular arrhythmias elicited by reperfusion<sup>50</sup>. In fact,  $K_{ATP}$  channel inhibition has been shown to prevent VF after acute myocardial infarction in non-insulin-dependent diabetic patients<sup>51</sup>. Furthermore,  $K_{ATP}$  channel inhibition effectively prevented arrhythmias induced by the combination of acute myocardial ischemia and exercise in dogs with healed myocardial infarctions<sup>50,52,53</sup>. Moreover, enhanced arrhythmogenicity related to  $K_{ATP}$  activation was confirmed in a recent study in explanted failing and non-failing human hearts<sup>54</sup>. Our experiments in monolayers of cardiomyocytes subjected to induction of metabolic sinks, by local perfusion with FCCP, supported this idea by showing that blocking sarcolemmal  $K_{ATP}$  channels blunted loss of APA and APD, and also, lowered the chance of reentry.

The findings of our experiments with FCCP-induced mitochondrial depolarization in the presence of  $K_{ATP}$  channel blockers supported the idea that  $K_{ATP}$  plays a major role in connecting mitochondrial dysfunction with electrical dysfunction of the cardiac tissue. However, when we investigated the effect of blocking  $K_{ATP}$  using glibenclamide (1, 10 or 20  $\mu$ M) or glimepiride (1  $\mu$ M) on coverslip-induced IR, we did not see any significant preventive effect on occurrence of mitochondrial oscillations. Also, in the presence of glibenclamide, 7 out of 8 monolayers showed post-ischemic reentry. This can be because the  $K_{ATP}$  blockers that we used might have also blocked mitochondrial  $K_{ATP}$  channels, causing loss of their protective effects against IR injury<sup>40,55</sup>. Also,  $K_{ATP}$  channels might



be acting as safety valves, which open, when the energy is low, to shut down cellular activities, and blocking them will cause extra stress on the cell. Furthermore, potency of  $K_{ATP}$  channel inhibition on IR injury and arrhythmogenesis is variable and very species-dependent. For example, in mice treated with the  $K_{ATP}$  channel blocker HMR1098, ischemia causes a much more rapid contracture of the isolated perfused heart (within 5 minutes of the onset of ischemia) compared to untreated hearts<sup>56</sup>. In this species, APs are already very short and the heart rate is extremely high (~600 bpm), which could potentially explain why  $K_{ATP}$  channel activation during ischemia is essential to prevent a tetanus-like depolarization of the membrane potential under metabolic stress. In contrast, in larger animals with slower heart rates and longer AP plateau potentials (e.g. guinea pig, dogs, and humans), glibenclamide treatment does not accelerate ischemic contracture, although it does prevent the protective effects of ischemic or chemical preconditioning<sup>42</sup>. These differences are largely due to differences in the electrophysiology of the cardiomyocytes of these species; e.g.,  $I_{to}$  is important in APD regulation in NRVM<sup>57</sup> but not in guinea pig heart cells. It should not be ignored that the electrophysiology of the cells in monolayer cultures of NRVMs is different from that of cardiomyocytes in intact heart, even in neonatal rats, let alone myocytes from other species. Moreover, differences in metabolism in adult versus neonatal hearts are well known, so while the NRVM monolayer is a practical and useful model to study electrical activity and mitochondrial function during IR, one should be careful not to generalize the results without caution and further experimentation. Nevertheless, the present work in NRVM monolayers strongly supports the hypothesis that mitochondrial  $\Delta\Psi_m$  instability

plays a major role in reperfusion arrhythmias, and that the mechanistic details underlying mitochondrial  $\Delta\Psi_m$  loss may be similar.

#### 4.1 Considerations

Mitochondrial depolarization and  $K_{ATP}$  activation are, undoubtedly, important contributors to cardiac cell dysfunction during IR injury; however, they represent only part of the spectrum of changes that happen in the myocardium during IR. Conditions of ischemia/reperfusion evoke a dramatic increase in  $I_{KATP}$ , but many other factors also come into play, including changes in transmembrane  $K^+$ ,  $Na^+$ , and  $Ca^{2+}$  gradients, pH, ATP,  $Mg^{2+}$ , as well as tissue conductivity. In fact, as the present experiments with the mitochondrial uncoupler show, mitochondrial  $\Delta\Psi_m$  collapse impacts the AP and the propagating wavefront in a manner that is more complex than expected simply from  $K_{ATP}$  channel activation and other effects of mitochondrial depolarization, such as CV slowing due to lower excitability, should be taken into account. Other factors such as increased dephosphorylation of Cx43 early during ischemia<sup>36</sup> might also contribute to CV slowing involved in arrhythmogenicity.

In the local perfusion studies, while we studied the effect of size of metabolic sink on the outcome, we did not have the freedom to move the sink to areas other than the center of the monolayer, or produce sinks with boundaries other than circular, due to limitations of the current design of our local perfusion system. Also, for optical mapping, using cameras with higher resolution and sensitivity could be very helpful for observing the dynamics of the activity in the sink (or ischemic) area.

In our experiments with coverslip-induced ischemia, the ischemic region regained excitability even after 70 minutes of ischemia, while a previous study by de Diego *et al.* reported that excitability did not recover after 25 minutes of ischemia<sup>36</sup>. This could be due to differences in materials used for cell culture or the coverslips; for example, whether the latter was glass or plastic, or the thickness and weight, which would affect the amount of media available to the ischemic region. Cell density or age of the monolayer could also contribute to the different outcomes.

In a monolayer, there is no fiber orientation-related anisotropy, and there are no connective tissues or blood vessels. There is no complex 3-dimensional structure that is seen in the whole heart either. These features make a monolayer a good model to study the electrophysiology of heart tissue at the syncytium level but it ignores higher order structural interactions. Differences related to the developmental stage of the cells may also come into play, as the ion channel and metabolic profile of neonates differs from the adult. Nevertheless, there is a rich literature supporting the use of such monolayers to study mechanisms of arrhythmias in the heart.

An additional concern is that the small size of the monolayer and the imposed boundary conditions of the coverslip are limitations that could affect the results. For example, in the case of reentrant waves, it is much easier for reentry to happen in a large tissue. The size of the excitable tissue with respect to the wavelength of propagation can affect the type of reentry or its sustainability. Therefore, in our experiments, we might be unable to see the exact type of reentrant behavior that happens in the whole heart; however, the results will be helpful to understand how insults at the level of mitochondria can change the activity

in a much bigger scale. To make a statement about the whole heart, we can use our results to design experiments in higher level models of the heart (wedges of heart tissue or whole perfused hearts).

## **4.2 Future Direction: Effect of Inhibition of Mitochondrial $\text{Na}^+/\text{Ca}^{2+}$ Exchanger on IR-Induced Reentry**

### **4.2.1 Objective and Methods**

Mitochondria are thought to play a major role in cytosolic  $\text{Ca}^{2+}$  overload and arrhythmogenesis during ischemia/reperfusion (IR) injury. The mitochondrial  $\text{Na}^+/\text{Ca}^{2+}$  exchanger (mNCE) plays a major role in control of  $[\text{Ca}^{2+}]_m$  and in tolerance to ischemia/reperfusion injury<sup>58</sup>.  $\text{Ca}^{2+}$  also plays a prominent role in NADH production by TCA cycle, which drives the electron transport chain and, consequently, ATP synthesis. Blocking  $\text{I}_{\text{NCE}}$  and therefore preventing  $\text{Ca}^{2+}$  extrusion from matrix can be protective against arrhythmias caused by heart failure<sup>59</sup>. Previously, it was shown that inhibition of mNCE using CGP-37157 increases mitochondrial  $\text{Ca}^{2+}$  ( $[\text{Ca}^{2+}]_m$ ) retention and prevents delayed afterdepolarizations and triggered arrhythmias during  $\text{Na}^+$  overload induced by the  $\text{Na}^+/\text{K}^+$  ATPase inhibitor ouabain *in vitro* and *in vivo*<sup>59</sup>. In isolated intact hearts, and in isolated cardiomyocytes as well, ouabain was used to increase  $[\text{Na}]_i$  and therefore to blunt  $\text{Ca}^{2+}$  accumulation inside mitochondria. Normally, it led to DAD and arrhythmias; however, adding CGP-37157 to block  $\text{I}_{\text{NCE}}$ , prevented these arrhythmias. Here, we investigated these findings in monolayers of cardiac myocytes. We studied the dynamics

of  $[Ca^{2+}]_m$  during coverslip-induced IR and investigated the role of mNCE in formation of IR-related reentry in NRVM monolayers. We looked at the effect of modifying  $I_{NCE}$  with CGP-37157, and applied novel gene transfer vectors to manipulate the levels of the putative mNCE protein NCLX<sup>60</sup> to determine if mNCE affects ischemia-related arrhythmias. Sarcolemmal electrical activity was recorded with a 464-photodiode array using the voltage-sensitive dye di-4-ANEPPS and changes in  $[Ca^{2+}]_m$  and cytosolic  $Ca^{2+}$  ( $[Ca^{2+}]_c$ ) were observed using the ratiometric genetically-encoded mitochondrial  $Ca^{2+}$  indicator GEM-GECO.

#### **4.2.2 Results and Conclusion**

Amplitude and conduction velocity of action potentials decreased over time until the ischemic region became inexcitable. During 1 hour of ischemia,  $[Ca^{2+}]_m$  increased in a sigmoidal fashion. Reperfusion of the monolayers with oxygenated Tyrode's solution lowered  $[Ca^{2+}]_m$  back to its initial value or even lower in less than 10 minutes (Figure 34).  $[Ca^{2+}]_c$  also increased during ischemia and, upon reperfusion, sharply decreased before increasing again later in the reperfusion phase (Figure 35).

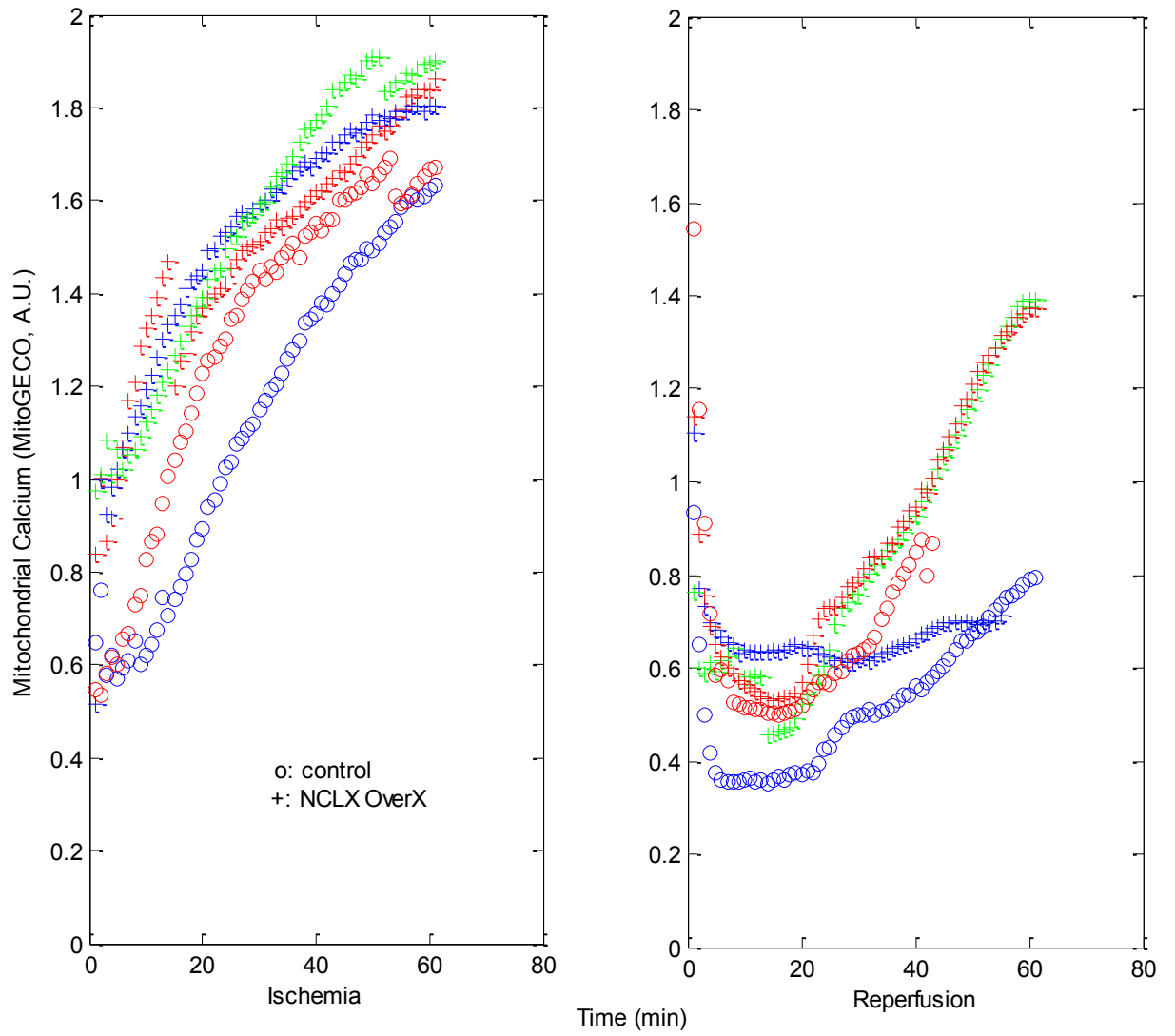
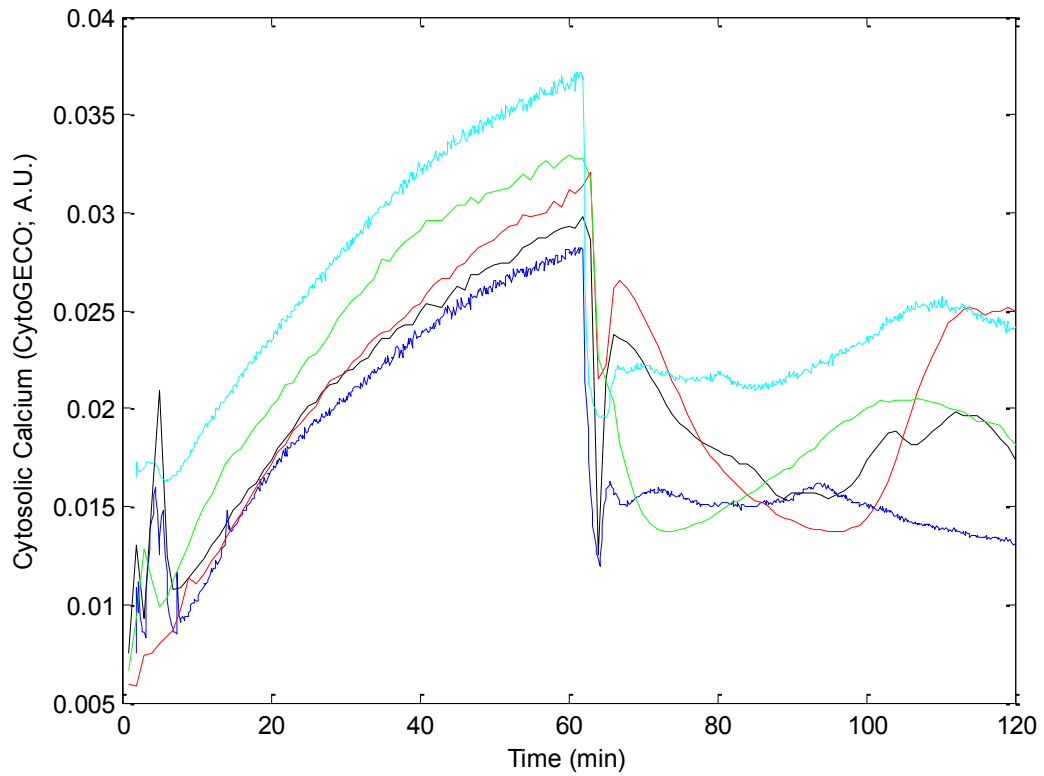


Figure 34  $[Ca^{2+}]_m$  during IR in control and NCLX-overexpressed monolayers.



**Figure 35  $[Ca^{2+}]_c$  during coverslip-induced IR.**

**Ischemia starts at time 0. Reperfusion starts at 60 minutes.**

To be sure that the changes in GECO signal are not a result of pH change due to IR, we looked at the pH change using SNARF, a ratiometric dye sensitive to pH. As seen in Figure 36, the dynamics of changes in pH are much faster than that of GECO. Also, GEM-CEGO is not very sensitive to pH in the range corresponding to IR conditions.

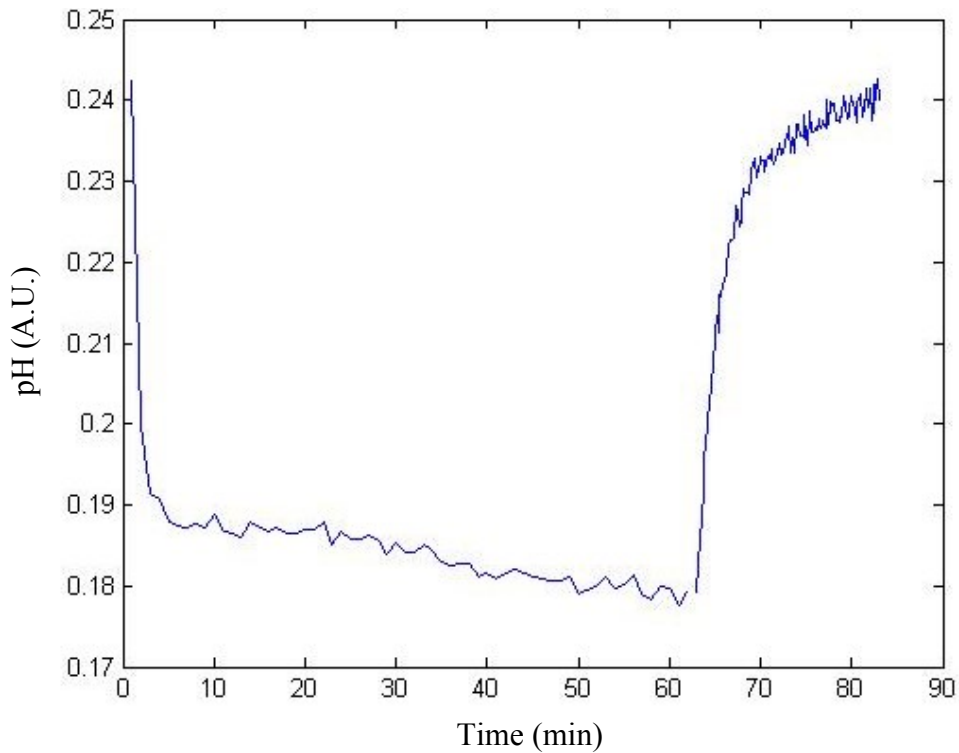


**Figure 36 Changes in the pH of the cardiac cells during IR.**

**Coverslip-induced IR: ischemia starts at 0 and reperfusion starts at 63 minutes.**

Wavelets and subsequently reentries formed upon reperfusion in 6 out of 7 monolayers. Presence of CGP-37157, at the concentration of  $1\mu\text{M}$ , in the media prevented or shortened the duration of wavelets and reduced the occurrence of reentries to 2 out of 5 monolayers (Figure 37). Viral overexpression of NCLX, the molecular candidate for mNCE, did not alter the incidence of reentry as compared to controls.



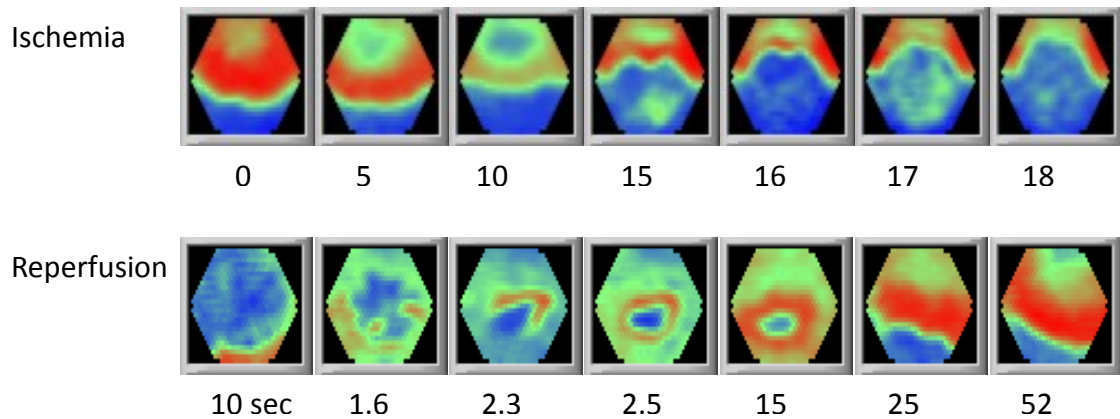


**Figure 37 Electrical activity of the monolayer in presence of CGP.**

**CGP (1  $\mu\text{M}$ ) prevents long-term reentry. Numbers beneath each figure, show the time in minutes.**

The results reveal the kinetics of  $[\text{Ca}^{2+}]_m$  during ischemia and reperfusion using a novel mitochondrial probe and demonstrate the cardioprotective effects of inhibition of mNCE. CGP-37157 decreased dispersion of repolarization and suppressed ischemia/reperfusion-related reentry.

### **4.3 Future Direction: Monolayers of Adult Cardiomyocytes**

We have also been using monolayer cultures of adult guinea pig myocytes as a potential experimental model for further investigation of present findings.

#### 4.4 Future Direction: Genetic Manipulation of Sarc-/Mito-K<sub>ATP</sub> Channels

Earlier, we described the importance of sarcolemmal K<sub>ATP</sub> channels in control of electrical activity of the cardiac myocytes. We observed some effects of chemically inhibiting these channels during FCCP perfusion and IR. For a better characterization of effects of sarc-K<sub>ATP</sub> channels, we have acquired shRNA viral vectors for knocking down this channel in our NRVM monolayers. Further experiments are designed and the model is under development.

The mitochondrial ATP-sensitive K<sup>+</sup> channel (mitoK<sub>ATP</sub>) has shown to be an important factor in cardio-protection against ischemia/reperfusion injury<sup>40,42</sup>. Mitochondrial ROMK channel is a molecular component of mitoK<sub>ATP</sub><sup>61</sup> and several gene transfer tools have been developed to overexpress or knock down the levels of this protein. We have started experiments to test mitochondrial ROMK's function by transducing monolayers of NRVMs with ROMK shRNA to determine if the presence of this channel plays an antiarrhythmic role in the context of coverslip-induced IR. We will compare this genetic manipulation approach to pharmacological inhibition of the channel (with 5-hydroxydecanoate). Similarly, we have been examining the effects of ROMK overexpression on susceptibility to ischemic electrical dysfunction and will compare the effects to those of pharmacological precondition via mitoK<sub>ATP</sub> channel activation with diazoxide.

## **Bibliography**

1. Donna L. Hoyert, Jiaquan Xu. Deaths: Preliminary data for 2011. *National vital statistics reports*. 2012;61(6).
2. Heidenreich PA, Trogon JG, Khavjou OA, et al. Forecasting the future of cardiovascular disease in the united states: A policy statement from the american heart association. *Circulation*. 2011;123(8):933-944.
3. Carry MM, Mrak RE, Murphy ML, Peng CF, Straub KD, Fody EP. Reperfusion injury in ischemic myocardium: Protective effects of ruthenium red and of nitroprusside. *Am J Cardiovasc Pathol*. 1989;2(4):335-44.
4. Maxwell SRJ, Lip GYH. Reperfusion injury: A review of the pathophysiology, clinical manifestations and therapeutic options. *Int J Cardiol*. 1997;58(2):95-117.
5. Wit AL, Janse MJ. Reperfusion arrhythmias and sudden cardiac death: A century of progress toward an understanding of the mechanisms. *Circulation Research*. 2001;89(9):741-743.
6. Lyon AR, Joudrey PJ, Jin D, et al. Optical imaging of mitochondrial function uncovers actively propagating waves of mitochondrial membrane potential collapse across intact heart. *J Mol Cell Cardiol*. 2010;49(4):565-575.
7. Slodzinski MK, Aon MA, O'Rourke B. Glutathione oxidation as a trigger of mitochondrial depolarization and oscillation in intact hearts. *J Mol Cell Cardiol*. 2008;45(5):650-660.

8. Aon MA, Cortassa S, Marban E, O'Rourke B. Synchronized whole-cell oscillations in mitochondrial metabolism triggered by a local release of reactive oxygen species in cardiac myocytes. *J Biol Chem*. 2003;278:44735-44744.
9. Zorov DB, Filburn CR, Klotz LO, Zweier JL, Sollott SJ. Reactive oxygen species (ROS)-induced ROS release: A new phenomenon accompanying induction of the mitochondrial permeability transition in cardiac myocytes. *J Exp Med*. 2000;192(7):1001-14.
10. Aon MA, Cortassa S, Maack C, O'Rourke B. Sequential opening of mitochondrial ion channels as a function of glutathione redox thiol status. *The Journal of biological chemistry*. 2007;282(30):21889-900.
11. Zhou L, Aon MA, Almas T, Cortassa S, Winslow RL, O'Rourke B. A reaction-diffusion model of ROS-induced ROS release in a mitochondrial network. *PLoS Comput Biol*. 2010;6(1).
12. Aon MA, Cortassa S, O'Rourke B. Percolation and criticality in a mitochondrial network. *Proc Natl Acad Sci U S A*. 2004;101(13):4447-52.
13. Beavis AD. On the inhibition of the mitochondrial inner membrane anion uniporter by cationic amphiphiles and other drugs. *J Biol Chem*. 1989;264(3):1508-15.
14. Beavis AD. Properties of the inner membrane anion channel in intact mitochondria. *J Bioenerg Biomembr*. 1992;24(1):77-90.

15. Sasaki N, Sato T, Marban E, O'Rourke B. ATP consumption by uncoupled mitochondria activates sarcolemmal K(ATP) channels in cardiac myocytes. *Am J Physiol Heart Circ Physiol*. 2001;280(4):H1882-8.
16. Zaitsev AV, Warren MD. Mechanisms of ischemic ventricular fibrillation. *Cardiac Electrophysiology: From Cell to Bedside (5th ed.)*, edited by Zipes DP and Jalife J. Philadelphia, PA: Saunders. 2009.
17. Hume J, Katzung BG. Physiological role of endogenous amines in the modulation of ventricular automaticity in the guinea-pig. *The Journal of physiology*. 1980;309:275-86.
18. Hauer RN, de Bakker JM, de Wilde AA, Straks W, Vermeulen JT, Janse MJ. Ventricular tachycardia after in vivo DC shock ablation in dogs. electrophysiologic and histologic correlation. *Circulation*. 1991;84(1):267-78.
19. Zeng J, Rudy Y. Early afterdepolarizations in cardiac myocytes: Mechanism and rate dependence. *Biophysical journal*. 1995;68(3):949-64.
20. Lederer WJ, Tsien RW. Transient inward current underlying arrhythmogenic effects of cardiotonic steroids in purkinje fibres. *The Journal of physiology*. 1976;263(2):73-100.
21. Panfilov A. Theory of reentry. *Cardiac Electrophysiology: From Cell to Bedside (5th ed.)*, edited by Zipes DP and Jalife J. Philadelphia, PA: Saunders. 2009.

22. Pandit SV, Jalife J. Rotors and the dynamics of cardiac fibrillation. *Circ Res.* 2013;112(5):849-862.
23. Aon MA, Cortassa S, Akar FG, O'Rourke B. Mitochondrial criticality: A new concept at the turning point of life or death. *BBA-Molecular Basis of Disease.* 2006;1762(2):232-240.
24. Aon MA, Cortassa S, O'Rourke B. The fundamental organization of cardiac mitochondria as a network of coupled oscillators. *Biophys J.* 2006;91(11):4317-4327.
25. Zorov DB, Juhaszova M, Sollott SJ. Mitochondrial ROS-induced ROS release: An update and review. *Biochimica et Biophysica Acta (BBA)-Bioenergetics.* 2006;1757(5):509-517.
26. Brady NR, Hamacher-Brady A, Westerhoff HV, Gottlieb RA. A wave of reactive oxygen species (ROS)-induced ROS release in a sea of excitable mitochondria. *Antioxidants & redox signaling.* 2006;8(9-10):1651-1665.
27. Kinnally KW, Zorov DB, Antonenko YN, Snyder SH, McEnery MW, Tedeschi H. Mitochondrial benzodiazepine receptor linked to inner membrane ion channels by nanomolar actions of ligands. *Proceedings of the National Academy of Sciences.* 1993;90(4):1374-1378.
28. Akar FG, Aon MA, Tomaselli GF, O'Rourke B. The mitochondrial origin of postischemic arrhythmias. *J Clin Invest.* 2005;115(12):3527-35.

29. Nicholls DG, Ferguson SJ, Ferguson S. *Bioenergetics*. Access Online via Elsevier; 2002.
30. Noma A. ATP-regulated K<sup>+</sup> channels in cardiac muscle. *Nature*. 1983;305(5930):147-8.
31. Lederer WJ, Nichols CG, Smith GL. The mechanism of early contractile failure of isolated rat ventricular myocytes subjected to complete metabolic inhibition. *The Journal of physiology*. 1989;413:329-49.
32. National Research Council. *Guide for the care and use of laboratory animals* <br />. 8th ed. Washington, DC: The National Academies Press; 2011.
33. Lin JW, Garber L, Qi YR, Chang MG, Cysyk J, Tung L. Region of slowed conduction acts as core for spiral wave reentry in cardiac cell monolayers. *American Journal of Physiology- Heart and Circulatory Physiology*. 2008;294(1):H58.
34. Davidson SM, Yellon D, Duchon MR. Assessing mitochondrial potential, calcium, and redox state in isolated mammalian cells using confocal microscopy. *METHODS IN MOLECULAR BIOLOGY-CLIFTON THEN TOTOWA-*. 2007;372:421.
35. Brown DA, Aon MA, Frasier CR, et al. Cardiac arrhythmias induced by glutathione oxidation can be inhibited by preventing mitochondrial depolarization. *J Mol Cell Cardiol*. 2010;48(4):673-679.

36. de Diego C, Pai RK, Chen F, et al. Electrophysiological consequences of acute regional ischemia/reperfusion in neonatal rat ventricular myocyte monolayers. *Circulation*. 2008;118(23):2330.
37. Pitts KR, Toombs CF. Coverslip hypoxia: A novel method for studying cardiac myocyte hypoxia and ischemia in vitro. *American Journal of Physiology- Heart and Circulatory Physiology*. 2004;287(4):H1801.
38. Griffiths EJ, Halestrap AP. Mitochondrial non-specific pores remain closed during cardiac ischaemia, but open upon reperfusion. *Biochem J*. 1995;307 ( Pt 1):93-8.
39. Hu H, Sato T, Seharaseyon J, et al. Pharmacological and histochemical distinctions between molecularly defined sarcolemmal KATP channels and native cardiac mitochondrial KATP channels. *Mol Pharmacol*. 1999;55(6):1000-1005.
40. Liu Y, Sato T, O'Rourke B, Marban E. Mitochondrial ATP-dependent potassium channels : Novel effectors of cardioprotection? *Circulation*. 1998;97(24):2463-2469.
41. Akao M, Ohler A, O'Rourke B, Marban E. Mitochondrial ATP-sensitive potassium channels inhibit apoptosis induced by oxidative stress in cardiac cells. *Circ Res*. 2001;88(12):1267-1275.
42. O'Rourke B. Evidence for mitochondrial K<sup>+</sup> channels and their role in cardioprotection. *Circ Res*. 2004;94(4):420-32.



43. Romashko DN, Marban E, O'Rourke B. Subcellular metabolic transients and mitochondrial redox waves in heart cells. *Proc Natl Acad Sci U S A*. 1998;95(4):1618-23.
44. Kuo CS, Amlie JP, Munakata K, Reddy CP, Surawicz B. Dispersion of monophasic action potential durations and activation times during atrial pacing, ventricular pacing, and ventricular premature stimulation in canine ventricles. *Cardiovascular research*. 1983;17(3):152-61.
45. O'Rourke B, Ramza BM, Marban E. Oscillations of membrane current and excitability driven by metabolic oscillations in heart cells. *Science*. 1994;265(5174):962-6.
46. Brown D, Aon M, Akar F, O'Rourke B. A ligand to the mitochondrial benzodiazepine receptor prevents ventricular arrhythmias and LV dysfunction after ischemia or glutathione depletion. *FASEB J*. 2008;22:747.7.
47. Brown DA, Aon MA, Akar FG, Liu T, Sorrairain N, O'Rourke B. Effects of 4'-chlorodiazepam on cellular excitation-contraction coupling and ischaemia-reperfusion injury in rabbit heart. *Cardiovascular research*. 2008;79(1):141-9.
48. Brown DA, Aon MA, Frasier CR, et al. Cardiac arrhythmias induced by glutathione oxidation can be inhibited by preventing mitochondrial depolarization. *Journal of Molecular and Cellular Cardiology*. ;In Press, Corrected Proof.

49. Kleber AG. Resting membrane potential, extracellular potassium activity, and intracellular sodium activity during acute global ischemia in isolated perfused guinea pig hearts. *Circulation research*. 1983;52(4):442-50.
50. Billman GE, Englert HC, Scholkens BA. HMR 1883, a novel cardioselective inhibitor of the ATP-sensitive potassium channel. part II: Effects on susceptibility to ventricular fibrillation induced by myocardial ischemia in conscious dogs. *J Pharmacol Exp Ther*. 1998;286(3):1465-73.
51. Lomuscio A, Vergani D, Marano L, Castagnone M, Fiorentini C. Effects of glibenclamide on ventricular fibrillation in non-insulin-dependent diabetics with acute myocardial infarction. *Coronary artery disease*. 1994;5(9):767-71.
52. Billman GE. The cardiac sarcolemmal ATP-sensitive potassium channel as a novel target for anti-arrhythmic therapy. *Pharmacology & therapeutics*. 2008;120(1):54-70.
53. Billman GE, Houle MS, Englert HC, Gogelein H. Effects of a novel cardioselective ATP-sensitive potassium channel antagonist, 1-[[5-[2-(5-chloro-o-anisamido)ethyl]-beta-methoxyethoxyphenyl]sulfonyl]-3-methylthiourea, sodium salt (HMR 1402), on susceptibility to ventricular fibrillation induced by myocardial ischemia: In vitro and in vivo studies. *The Journal of pharmacology and experimental therapeutics*. 2004;309(1):182-92.

54. Fedorov VV, Glukhov AV, Ambrosi CM, et al. Effects of K<sup>+</sup> ATP channel openers diazoxide and pinacidil in coronary-perfused atria and ventricles from failing and non-failing human hearts. *J Mol Cell Cardiol.* 2011;51(2):215-225.
55. O'Rourke B. Myocardial KATP channels in preconditioning. *Circ Res.* 2000;87(10):845-855.
56. Suzuki M, Saito T, Sato T, et al. Cardioprotective effect of diazoxide is mediated by activation of sarcolemmal but not mitochondrial ATP-sensitive potassium channels in mice. *Circulation.* 2003;107(5):682-5.
57. Kassiri Z, Zobel C, Molkentin JD, Backx PH. Reduction of Ito causes hypertrophy in neonatal rat ventricular myocytes. *Circ Res.* 2002;90(5):578-585.
58. Griffiths EJ, Halestrap AP. Protection by cyclosporin A of ischemia/reperfusion-induced damage in isolated rat hearts. *J Mol Cell Cardiol.* 1993;25(12):1461-1469.
59. Liu T, Brown DA, O'Rourke B. Role of mitochondrial dysfunction in cardiac glycoside toxicity. *J Mol Cell Cardiol.* 2010;49(5):728-736.
60. Palty R, Silverman WF, Hershinkel M, et al. NCLX is an essential component of mitochondrial Na<sup>+</sup>/Ca<sup>2+</sup> exchange. *Proceedings of the National Academy of Sciences.* 2010;107(1):436-441.
61. Foster DB, Ho AS, Rucker J, et al. Mitochondrial ROMK channel is a molecular component of MitoKATP. *Circulation Research.* 2012;111(4):446-454.

## **Curriculum Vitae**

### **Education History**

Ph.D.            2013    Biomedical Engineering        Johns Hopkins School of Medicine

Mentor: Brian O'Rourke

M.Sc.           2005    Biomedical Engineering        Amirkabir University of Technology

Mentor: Reza Hashemi Golpayegani

B.Sc.           2002    Biomedical Engineering        Shahed University

### **Other Professional Experiences**

Researcher            2004-2005    Research Center for Intelligent Signal Processing

Instructor            2004            Microcomputer Laboratory, Shahed University

Volunteer Instructor    2004            Programming in MATLAB, Amirkabir University  
of Technology

Volunteer Instructor    2002            Programming in MATLAB, Shahed University

Intern            2002            Repair and Maintenance Dept, Iranian Company of  
Distribution of Medical Products

Intern            2001            Medical Equipment Dept, Namazi Hospital, Shiraz, Iran

### **Scholarships, fellowships, or other external funding**

4 NHLBI Travel Awards    2009-2011    National Heart, Lung, and Blood Institute,  
National Institute of Health

2 SAMSI Travel Awards    2008            Statistical and Applied Mathematical  
Sciences Institute

### **Peer-Reviewed Publications (Papers/Abstracts)**

**S Solhjo**, B O'Rourke, Effect of Regional Ischemia-Reperfusion on Mitochondrial  
Function and Electrical Propagation in NRVM Monolayers, [Under preparation]

L Zhou\*, **S Solhjo**\*, B Millare, G Plank, MR Abraham, S Cortassa, N Trayanova, B  
O'Rourke, Effects of Regional Mitochondrial Depolarization on Electrical Propagation:  
Implications for Arrhythmogenesis, [*under review*]

**S Solhjoo**, B O'Rourke (2013) Mitochondrial Inner-Membrane Potential Instability Promotes Sarcolemmal Electrical Instability after Ischemia-Reperfusion in Monolayers of Cardiac Myocytes, *Circulation Research*. 2013;113:A332

L Zhou, **S Solhjoo**, G Plank, MR Abraham, S Cortassa, N Trayanova, B O'Rourke (2011) Regional Mitochondrial Depolarization Causes Spontaneous Ventricular Arrhythmia in Cardiac Tissue, *Biophysical Journal* 100:3, Supplement 1, pp. 435a-436a

L Zhou, **S Solhjoo**, G Plank, S Cortassa, MR Abraham, N Trayanova, B O'Rourke (2010) Emergent Ventricular Fibrillation caused by Regional Mitochondrial Depolarization in Cardiac Muscle, *Circulation* 122:A20902

**S Solhjoo**, MR Abraham, B O'Rourke (2010) Effect of Regional Mitochondrial Uncoupling on Electrical Propagation in Cardiac Cell Monolayers, *Biophysical Journal* 98:3, Supplement 1, p. 527a

**S Solhjoo**, AM Nasrabadi, MH Golpayegani (2005) EEG-Based Mental Task Classification in Hypnotized and Normal Subjects, 27th Annual International IEEE-EMBS Conference of the Engineering in Medicine and Biology Society, pp. 2041-2043

A Akrami, **S Solhjoo**, AM Nasrabadi, MH Golpayegani (2005) EEG-Based Mental Task Classification: Linear and Nonlinear Classification of Movement Imagery, 27th Annual International IEEE-EMBS Conference of the Engineering in Medicine and Biology Society, pp. 4626-4629

**S Solhjoo**, AM Nasrabadi, MH Golpayegani (2005) Classification of Chaotic Signals Using HMM Classifiers: EEG-Based Mental Task Classification, 13th European Signal Processing Conference EUSIPCO2005, pp. -

**S Solhjoo**, MH Moradi (2004) Mental Task Recognition: A Comparison between Some of Classification Methods, BIOSIGNAL 2004 International EURASIP Conference, pp. 24–26

**S Solhjoo**, MH Golpayegani, AM Nasrabadi (2004) Modeling of Parkinson's Disease Considering Different Causes Producing Parkinsonian Effects, BIOSIGNAL International EURASIP Conference, pp. 396–398

**S Solhjoo**, MH Moradi (2004) Local Neural Classifier in Mental Tasks Recognition, 11th Iranian Conference on Biomedical Engineering (ICBME2004), pp. -

**S Solhjoo**, MH Golpayegani, AM Nasrabadi (2004) Modeling of Parkinson's Disease, 11th Iranian Conference on Biomedical Engineering (ICBME2004), pp. -

**S Solhjoo**, MA Khalilzadeh (2003) Hemodynamic Parameters Estimation, Using Electrical Admittance of Chest [in Farsi], 6th Iranian Students Conference on Electrical Engineering

**S Solhjoo**, M Darainy (2003) The Relation between Control Horizon, Prediction Horizon, and Model Error in Model Predictive Impedance Control (MPIC) of Elbow Joint [in Farsi], 6th Iranian Students Conference on Electrical Engineering

## **Service and Leadership**

2010-2012 Representative for "Student Assistance Program," at the Graduate Student Association

2009 Teaching Assistant for "Cell and Tissue Engineering Lab"

2008 Teaching Assistant for "Modeling and Design"